Industrial Crops & Products 233 (2025) 121382

Contents lists available at ScienceDirect

Industrial Crops & Products

journal homepage: www.elsevier.com/locate/indcrop

Enhanced production of novel bioactive metabolites in mung bean (*Vigna radiata* (L.) R. Wilczek) plants induced by signal molecule ethylene in a vertical farm

Du Yong Cho [a,1], Se Hyeon Jeon [b,1], Mu Yeun Jang [a], Eun Jeong Ko [b], Hee Yul Lee [a,c], Jong Bin Jeong [a], Ga Yong Lee [a], Ki-Ho Son [a], Md. Azizul Haque [d], Jin Hwan Lee [b,*], Kye Man Cho [a,*]

[a] Department of GreenBio Science and Agri-Food Bio Convergence Institute, Gyeongsang National University, Jinju 52727, Republic of Korea
[b] Department of Smart Green Resources, Dong-A University, 37, Nakdong-Daero 550 Beon-gil, Saha-gu, Busan 49315, Republic of Korea
[c] Gyeongnam Anti-Aging Research Institute, Sancheong-gun, Gyeongsangnam-do 52215, Republic of Korea
[d] Department of Biochemistry and Molecular Biology, Hajee Mohammad Danesh Science and Technology University, Dinajpur 5200, Bangladesh

ARTICLE INFO

Keywords:
mung bean
metabolite farming
ethylene
isoflavone
flavone
DNA protection

ABSTRACT

In the biofunctional material industry, enhancing bioactive metabolites in plants using signal stimulants is an emerging strategy. This study investigated the changes in bioactive metabolite content in different organs of mung bean plants treated with ethylene (ETL) in a closed chamber. In addition, we also examined its biomass, novel compounds, biological activities, and DNA protection. Through this approach, a practical method for producing mung bean plants with enhanced bioactive metabolites was proposed. ETL treatments led to a notable reduction in biomass, particularly in the leaves and roots, without affecting plant height. ETL treated leaves exhibited significant increases in the total phenolic, flavonoid, isoflavone, and flavone contents. Four compounds were identified in the mung bean organs following ETL treatment: 2′-hydroxydaidzein-4′,7-*O*-diglucoside, daidzein-4′,7-*O*-diglucoside, 2′-hydroxydaidzin, and 2′-hydroxydaidzein. Among these isoflavones, 2′-hydroxydaidzin and daidzin showed the highest significant accumulation levels in ETL treated leaves. In particular, the contents of 2′-hydroxydaidzin, daidzin, and genistin in the ETL treated leaves was increased by 77.4-fold (273.24–21,159.88 μg/g), 74.2-fold (429.67–31,845.13 μg/g), and 12.0-fold (268.35–3209.12 μg/g) respectively, compared with their contents in untreated leaves. Furthermore, the total phenolic and flavonoid contents increased from 13.87–24.59 and from 9.89 to 12.87 mg/g, respectively. These enhanced active metabolites in ETL treated mung bean organs significantly improved the antioxidant capacity, including radical scavenging, digestive enzyme-inhibition, and DNA protection activities. These findings underscore the potential of ETL as an effective elicitor and enhancer of bioactive metabolite production, supporting its application in high value functional bioresources.

1. Introduction

Metabolite farming is an agricultural and biotechnological technique aimed at increasing or optimizing specific plant metabolites, which are used in functional materials, pharmaceuticals, cosmetics, or industrial applications (Lee et al., 2024a; Tripathi et al., 2024; Selwal et al., 2023). This technique concentrates on secondary metabolites that plants release in response to environmental stress or as defense mechanisms (Tripathi et al., 2024; Dubois et al., 2018; Pisoschi and Pop, 2015). Secondary metabolites encompass various bioactive compounds, such as flavonoids, isoflavones, alkaloids, and terpenoids, which are essential for human health and offer significant benefits, such as antioxidant,

Abbreviations: 2HDAEDG, 2'-hydroxydaidzein-4′,7-*O*-diglucoside; 2HDAE, 2'-hydroxydaidzein; 2HDAI, 2'-hydroxydaidzin; DAI, daidzin; DAE, daidzein; DAEDG, daidzein-4′,7-*O*-diglucoside; VTX, vitexin; IVTX, isovitexin; GEE, genistein; GEI, genistin; GLE, glycitein; TF, total flavonoid; TP, total phenolic; GLI, glycitin; SD, seed; GM, germination; CTL, control; ETL, ethylene; HPLC, high-performance liquid chromatography; LIN, linear DNA; OC, open circular DNA; SC, supercoiled DNA.

* Corresponding authors.
E-mail addresses: schem72@dau.ac.kr (J.H. Lee), kmcho@gnu.ac.kr (K.M. Cho).

[1] These authors made equal contributions to this work.

https://doi.org/10.1016/j.indcrop.2025.121382
Received 4 April 2025; Received in revised form 14 June 2025; Accepted 16 June 2025
Available online 19 June 2025

anti-inflammatory, and anticancer properties (Banwo et al., 2021). Notably, the production of these metabolites is regulated by phytohormones (Mcsteen and Zhao, 2008). Studies indicated that phytohormones can enhance agricultural productivity, improve environmental stress tolerance, and significantly affect metabolite synthesis (Kim et al., 2023; Kim et al., 2022; Li et al., 2013). In particular, enhancing the bioactive metabolites contained in small quantities in plants than by increasing plant biomass is more economically beneficial in metabolic farming (Lee et al., 2024a; Kim et al., 2023).

Ethylene (ETL) is a gas phytohormone that influences physiological processes such as fruit ripening, leaf senescence, and stomatal closure (Dubois et al., 2018). Specifically, through cell signaling pathways, ETL regulates plant physiologic and metabolic activities by activating the synthesis of stress-induced defense proteins and secondary metabolites (Gupta et al., 2018a; Gupta et al., 2018b). Interestingly, these properties offer significant potential. The intake of ETL treated soybean leaves was found to alleviate cognitive impairment and osteoprotective effects by promoting phytoestrogen and amino acid synthesis (Lee et al., 2023; Yoo et al., 2022; Ban et al., 2021; Ban et al., 2020; Xie et al., 2020). Furthermore, the roots of *Angelica accutiloba* stimulated furanocoumarin production, which increased its monoamine oxidase inhibition activity (Lee et al., (2024a) In addition to the increased levels of metabolites that amplify stress resistance in these plants, bioactive metabolites with enhanced biofunctional materials may be developed through bioprocessing (Lee et al., 2024b). This will further expand the potential for commercial utilization as a high value bioresource.

Isoflavones are phytochemicals abundantly found in legume crops such as soybeans and mung beans (*Vigna radiata* (L.) R. Wilczek). They are known as phytoestrogens due to their structural and functional resemblance to the female hormone estrogen (Lee et al., 2024c; Shen et al., 2022; Kim, 2021; Petrine et al., 2020; Bai et al., 2016). The main isoflavones are the derivatives of daidzin (DAI), glycitin (GLI), genistin (GEI), daidzein (DAE), glycitein (GLE), and genistein (GEE). These isoflavones are bioactive metabolites with various health benefits (Lee et al., 2024b; Kim, 2021), and are associated with the prevention of menopause, osteoporosis, cardiovascular diseases, neuroprotection, and cancer (Petrine and Del Bianco-borges, 2020). Flavones, a class of polyphenolics widely distributed in plants, also exhibit numerous bioactive properties (Chagas et al., 2022; Shen et al., 2022). Apigenin (AGN), a representative flavone compound, exists in glucoside forms such as vitexin (VTX) and isovitexin (IVTX) (Li et al., 2024; Chagas et al., 2022). These compounds are also abundant in plants such as green tea, parsley, celery, chamomile, and mung beans (Li et al., 2024; Shen et al., 2022; Bai et al., 2017; Bai et al., 2016). Flavone derivatives are recognized for their significant antioxidant, anti-inflammatory, and neuroprotective roles (Chagas et al., 2022; He et al., 2016), rendering isoflavones and flavones as the focal areas for nutraceutical research.

Antioxidants are compounds that scavenge reactive oxygen species (ROS) and free radicals, which cause cellular damage and oxidative stress (Kim, 2021; Juan et al., 2021; Ganesan and Xu, 2017). Among these compounds, plant-derived bioactive metabolites, like polyphenols, flavonoids, and isoflavones, scavenge free radicals and chelate transition metals, which are implicated in oxidative damage (Kim et al., 2023; Khole et al., 2016; Xiao et al., 2016; Silva et al., 2013). A recent study suggested that the plant treatment of inducers (e.g., ETL, salicylic acid, and abscisic acid), which enhances the production of bioactive metabolites, promotes radical scavenging and enzyme-inhibition activities (Lee et al., 2024a; Lee et al., 2023; Kim et al., 2023; Li et al., 2013). This method not only elucidates improved antioxidant efficacy and DNA protection but also implies the potential for the conversion of agricultural residues into a high-value bioresource (Lee et al., 2023; Kalim et al., 2010). These agricultural residues can increase resource efficiency and help in achieving sustainable agriculture (Leite Milião et al., 2022).

This study aimed to produce new isoflavone derivatives from ETL treated mung bean plants that were not identified in previous studies on isoflavone-enriched soybean leaves (Lee et al., 2023; Ban et al., 2020). Additionally, the *in vitro* biological activities, including radical scavenging, digestive enzyme-inhibition, and DNA protection effects, were examined to clarify the potential of these metabolites as bioactive compounds. The results suggest the potential use of agricultural residues such as leaves, stems, and roots as biofunctional materials and value-added bioresources.

2. Materials and methods

2.1. Chemicals, reagents, and instruments

The standard products used in this study were isoflavone and flavone derivatives such as DAI, GLI, GEI, DAE, GLE, GEE, VTX, IVTX, and AGN, which were purchased from Sigma-Aldrich Chemical Co. (St. Louis, MO, USA). As previously described, the reagents used for *in vitro* biological activity, total phenolics (TP), and total flavonoids (TF) were purchased from Sigma-Aldrich·H_2O, MeOH, EtOH, and acetonitrile (ACN) were purchased from J.T. Baker (Phillipsburg, NJ, USA) which were used as analysis and extraction solvents. The instrument used in the study was high-performance liquid chromatography (HPLC, Agilent 1200 series, Agilent Co. Forest Hill, Big, USA) to analyze isoflavones and flavones. A spectrophotometer (Shimadzu UV-1800, Nakagyo-ku, Kyoto, Japan) was used for the TP and TF analyses. An ELISA microplate reader (ELX800, Bio-Tek Instruments, Inc., Winooski, VT, USA) was used to measure the *in vitro* biological activity. DNA protection was conducted by electrophoresis (Mupid-exU, Takara Bio Inc., Japan) and UV transilluminators (BioDoc-It™ 220 imaging system, Analytik Jena, Jena, Germany). ^{1}H- and ^{13}C nuclear magnetic resonance (NMR) data (500 and 125 MHz) of the isolated DAE derivatives were obtained using a Bruker AM 500 NMR spectrometer (Karlsruhe, Land Baden-Württemberg, Germany) in DMSO-d_6 with tetramethyl as the internal standard. Preparative HPLC was performed on a versatile HPLC system (LC-Forte/R-II, YMC Corporation, Kyoto, Japan) equipped with a preparative ODS-A column (YMC-Triart C18, 250 × 20 mm I.D., YMC Co., Japan).

2.2. Experimental design

2.2.1. Plant materials and growth conditions

Mung bean seeds (SDs) were provided by the Korea Partnership for Innovation of Agriculture (KOPIA, Jeonju, Korea) in 2023 and stored at 4°C (Fig. 1A). The SDs were immersed in 2 % sodium hypochlorite for 1 min and then washed with distilled water (DW). Sterilized SDs were immersed in DW and germinated (GM) for 24 ± 1 h at 25°C in the dark (Fig. 1B). The GM mung beans were transplanted into flowerpots containing raised bed soils (pH 4.0–7.0, EC 1.2 dS/m, Pungnong Co., Ltd., Korea). The twenty-four flowerpots were placed in plastic containers (W × L × H, 540 × 275 × 60 mm). The plants were grown in a container-vertical farm system (Fig. S1) under a temperature of 25 ± 2°C, relative humidity of 50 % ± 10 %, and light intensity of 143.68 $\mu mol \cdot m^{-2} \cdot s^{-1}$ (photoperiod of 16 h; LED T5–1200L-HC, Dongyoung Co. Ltd., Korea). The growth conditions were maintained for 28 days (Fig. 1C and D).

2.2.2. Ethylene (ETL) treatment conditions

Mung bean plants were treated with ETL according to the method of Lee et al. (2023), with slight modifications in a smart-metabolite chamber (Fig. S2). After creating a sealed environment for the smart-metabolite chamber before ETL treatment, the temperature (25 ± 2°C) and light intensity (142.29 $\mu mol \cdot m^{-2} \cdot s^{-1}$; photoperiod of 16 h) were maintained consistent with the conditions of the container-vertical farm system, and the humidity was maintained at 90 % ± 5 %. Mung bean plants were treated with ETL at 10,000 ppm twice (every 24 h) for 48 h. The final mung bean plants were divided into control (CTL, untreated ETL) and ETL groups (Fig. 1E and F).

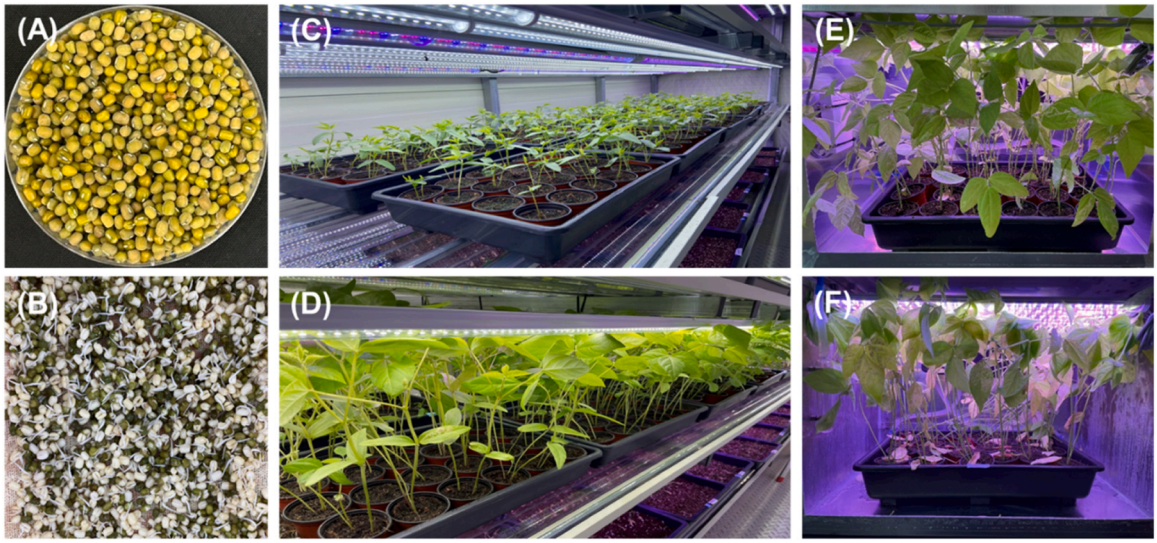

Fig. 1. Photographs of mung bean cultivation and ethylene treatment. (A) seed; (B) germination; (C) grown 14 days; (D) grown 28 days; (E) untreated by ethylene; and (F) treated with ethylene.

2.3. Length and biomass measurement

After 28 days of sowing, the length and fresh and dry weights of ETL treated and untreated mung bean plants were measured by randomly selecting 10 plants. Plant length was measured using a digital vernier caliper (552–304–10, Mitutoyo Corp., Kawasaki, Japan), defined as the maximum length (cm) from the top cotyledon to the root tip. Fresh weight was recorded using an electronic balance (HS2200S, Hansung Instrument Co., Ltd, Seoul, Korea) after separating the plant organs into leaves, stems, and roots. Then, the dry weight was recorded after maintaining the plant in a dry oven (WOF-W155, DAIHAN Scientific Co., Ltd., Wonju, Korea) at 50°C for 48 h. Unpaired t-tests using GraphPad (version 8.2.1, La Jolla, CA, USA) were conducted to identify significant differences in the effect of ETL treatments.

2.4. Extraction and isolation of DAE standards

Four DAE derivatives were isolated using column chromatography and preparative HPLC, as previously described (Ha et al., 2021; Kim et al., 2020). The ETL treated pulverized mung bean whole plant (2 kg) was extracted with 50 % MeOH (3 L × 4) in a shaking incubator for 7 days at room temperature. The combined 50 % methanol extract was concentrated using a rotary evaporator at 40°C to yield dark green gum. The resulting residue (210 g) was chromatographed on silica gel (15 × 60 cm, 230 −400 mesh, 980 g) using $CHCl_3$-acetone (v/v) [20:1 (1.5 L) → 15:1 (1.2 L) → 10:1 (1.2 L) → 7:1 (1.2 L) → 5:1 (1 L) → 2:1 (1 L) → 1:1 (1 L)] and $CHCl_3$-MeOH (v/v) [12:1 (1 L) → 8:1 (1 L) → 6:1 (1 L) → 4:1 (1 L) → 2:1 (1 L) → 1:1 (1 L) → 1:3 (1 L)] mixtures to give 65 fractions (F1 −F65). Fractions F26 −F28 (1.3 g) were further fractionated by silica gel column chromatography (2.5 × 45 cm, 230 −400 mesh, 35 g) with $CHCl_3$-acetone (10:1 → 1:2, v/v) to afford 32 subfractions. Based on the comparison of the thin layer chromatography (TLC) patterns, subfractions 25 −28 (105 mg) were evaporated and chromatographed on silica gel (1.2 × 25 cm, 230 −400 mesh, 16 g) with $CHCl_3$-acetone (3:1 → 1:2, v/v) to yield compound **9** (18 mg). Fractions F47 −F52 (5.9 g) were chromatographed on a silica gel column (4.5 × 50 cm, 230 −400 mesh, 105 g) using a gradient of $CHCl_3$-MeOH starting at 18:1, with the polarity increasing to a final ratio of 1:2 to produce 49 subfractions. Subfractions 17 −20 (430 mg) were subjected to medium-pressure liquid chromatography using a gradient elution of CH_3CN in water (5 → 45 %, 19 mL/min) and then purified by Sephadex LH-20 (50 % MeOH), yielding compound **3** (37 mg). Subsequently, subfractions 36 −41 (790 mg) were chromatographed on a Sephadex LH 20 column (1.5 × 70 cm, 45 g) using 50 % MeOH, from which compound **2** (21 mg) was obtained. In the above separation process, the elution fractions containing major compound **1** and minor compound **2** were rechromatographed on Sephadex LH-20 with 90 % MeOH and purified with preparative TLC ($CHCl_3$:MeOH = 1:1) to give compound **1** (15 mg).

2.5. Sample extraction

Here, 1 g and 10 mL of each sample and 50 % MeOH were mixed in a conical tube. The mixture was subjected to stirring extraction at 25°C ± 2°C for 24 h. The mixed extracts were centrifuged at 3000 × g for 10 min. Then, the extract supernatants passed through a membrane filter (0.45 μm, Whatman plc., Little Chalfont, Buckinghamshire, UK). These 50 % MeOH extracts of mung bean organs were used to analyze the HPLC, *in vitro* biological activity, and DNA protection.

2.6. Analysis of bioactive metabolites

2.6.1. Analysis of NMR spectroscopy

Four DAE derivatives (**1**–**3** and **9**) were dissolved in a deuterated solvent (DMSO-d_6) with tetramethylsilane (TMS) as the internal standard, using 5 mm NMR tubes (Bai et al., 2016; Ha et al., 2021). NMR spectra were acquired to determine chemical shifts relative to TMS. The spectral data included one-dimensional (^{1}H and ^{13}C), DEPT-90/135, and two-dimensional NMR techniques, such as ^{1}H–^{1}H COSY and HSQC. All chemical shift values were reported in parts per million (ppm), and the coupling constants (*J*) were reported in Hertz (Hz), as previously described (Ha et al., 2021). Data acquisition and processing were performed using XWINNMR software (version 2.1; Bruker, Rheinstetten, Germany) on a Silicon Graphics O_2 workstation. The structural elucidation of four DAE derivatives was conducted based on their NMR spectral features, molecular ion masses, and comparison with previously reported data (Fujitaka et al., 2019; Bai et al., 2016; Yoo et al., 2004; Kobayashi and Ohta, 1983).

2.6.2. Analysis of isoflavones and flavones with HPLC

The isoflavone and flavone contents of the mung bean organ extracts were evaluated toward 13 standards (Fig. 2). The isoflavone and flavone contents were analyzed using HPLC equipped with a LiChropper 100 RP-18 column (4.6 × 250 mm, 5 μm) and a diode array detector (1260

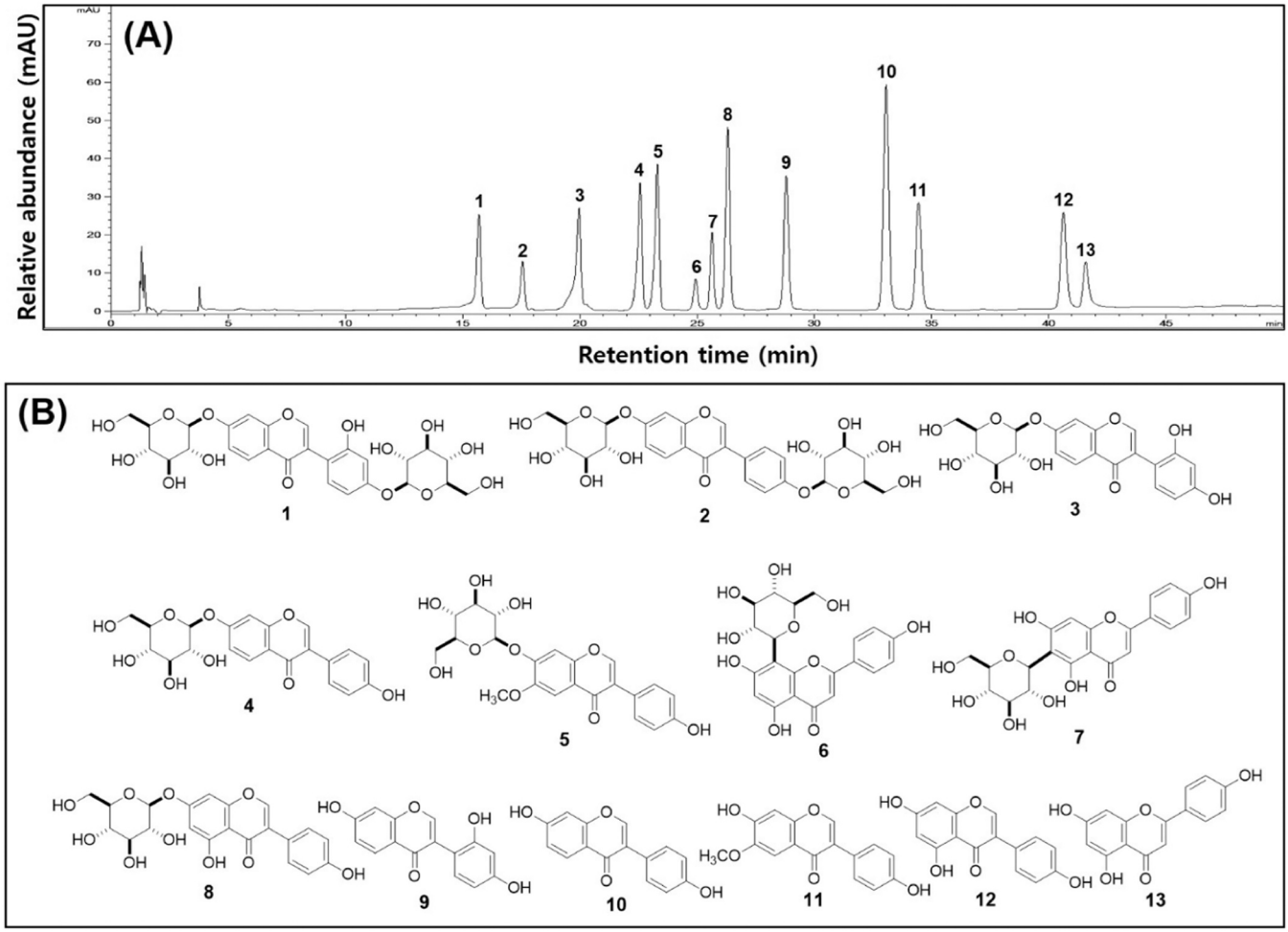

Fig. 2. Typical HPLC chromatograms and chemical structures of 10 isoflavone and 3 flavone derivatives. (A) Typical HPLC chromatograms and (B) chemical structures. 13 Chemicals: 1, 2′-hydroxydaidzein-4′,7-*O*-diglucoside (2HDAEDG); 2, daidzein-4′,7-O-diglucoside (DAEDG); 3, 2′-hydroxydaidzin (2HDAI); 4, daidzin (DAI); 5, glycitin (GLI); 6, vitexin (VTX); 7, isovitexin (IVTX); 8, genistin (GEI); 9, 2′-hydroxydaidzein (2HDAE); 10, daidzein (DAE); 11, glycitein (GLE); 12, genistein (GEE); and 13, apigenin (AGN).

series, Agilent Co. Forest Hill, Big, USA). The HPLC analytical settings were set at an injection volume of 20 μL, column temperature of 30 °C, and absorbance of 254 nm. The analytical solvent was H_2O containing 0.2 % acetic acid (solvent A) and ACN containing 0.2 % acetic acid (solvent B), with the gradient conditions set to solvent B: 15 min, 0 %–10 %; 25 min, 10 %–20 %; 35 min, 20 %–25 %; 45 min, 25 %–35 %; and 50 min, 35 % (Lee et al., 2024b). Each sample's isoflavone and flavone contents were quantified by comparing the retention durations with those of the appropriate standard molecule. Isoflavone and flavone standards were quantified by dissolving them in DMSO and using a linear calibration curve of each standard, with a coefficient of determination (R^2) > 0.998. The calibration curve was set to seven points (6.25, 12.5, 25, 50, 100, and 200 μg/mL) for each standard.

2.6.3. Measurement of TPs

The TP contents were measured using the method described by Lee et al. (2024b). Initially, the sample extracts (500 μL) and 25 % Na_2CO_3 (500 μL) were placed in a test tube and allowed to stand for 3 min. Then, 2 N Folin–Ciocalteu's phenol reagent (250 μL) was mixed and reacted at 30°C for 1 h. Next, the optical density (OD) of the solution was measured using a spectrophotometer (Shimadzu UV-1800, Nakagyo-ku, Kyoto, Japan) at 750 nm. The TP contents were calculated by preparing a standard curve (R^2 = 0.998) using gallic acid standard solutions (100, 50, 25, 12.5, and 6.25 μg/mL).

2.6.4. Measurement of TFs

The TF contents were measured according to the method described by Lee et al. (2024b). Initially, 500 μL of the sample extracts and 1000 μL ethylene-glycol were mixed in a test tube. Then, 10 μL of 1 M NaOH was added and reacted at 37°C for 1 h. Thereafter, the OD of the solution was recorded using a spectrophotometer at 420 nm. The TF contents were calculated by preparing a standard curve (R^2 = 0.997) using rutin standard solutions (100, 50, 25, 12.5, and 6.25 μg/mL).

2.7. In vitro biological activity analysis

The DPPH and ABTS radical scavenging, as well as α-glucosidase and pancreatic-lipase-inhibition activities of the mung bean extracts, were investigated using previously described methods (Lee et al., 2024b). To evaluate the DPPH radical scavenging activity, a 96-well microplate was filled with 40 μL of the sample extracts and 160 μL of 1.5×10^{-4} M DPPH MeOH solution. The mixture was homogenized and left in the dark at 30°C for 30 min. Then, the OD of the solution was measured at 515 nm using a microplate reader. To evaluate the ABTS radical scavenging activity, 20 μL of the sample extracts and 180 μL of the ABTS radical solution were mixed and left in the dark at 30°C for 3 min. The OD of the solution was then measured at 730 nm. To evaluate the α-glucosidase inhibition activity, 10 μL of the sample extracts were mixed with 20 μL of the 1 U/mL α-glucosidase enzyme solution and 20 μL of 0.01 M ρ-nitrophenol-α-D-glucopyranoside. The mixture was

then incubated at 37°C for 20 min and then stopped with 150 μL of 0.1 M Na_2CO_3. The OD of the solution was measured at 420 nm. To evaluate the pancreatic-lipase-inhibition activity, 10 μL of the sample extracts and 20 μL of 1 U/mL lipase enzyme solution were mixed with 20 μL of 0.01 M ρ-nitrophenyl butyrate. Then, the mixture was incubated at 37°C for 20 min and then stopped with 150 μL of 0.1 M Na_2CO_3. The OD of the solution was measured at 420 nm. The IC_{50} value was derived from serial concentration measurements using GraphPad software (version 8.2.1, La Jolla, CA, USA).

2.8. Oxidative DNA damage protection analysis

The DNA-protecting effects of mung bean extracts from hydroxyl radicals were evaluated *in vitro* using supercoiled DNA (SC, pGEM-T Easy from *Escherichia coli*) as investigated previously (Lee et al., 2024d). Plasmid DNA was extracted using 1 × TE buffer (10 mM Tris-HCl and 1 mM EDTA as elution buffer, pH 7.4) and Fenton's reagent (100 mM H_2O_2, 0.1 mM acetic acid, and 1.6 mM $FeCl_3$). Initially, 2 μL of pBluescript SK(+) vector, 10 μL of mung bean sample extracts, and 8 μL of Fenton's reagent were incubated at 30°C for 1 h. Then, 25 mg of bromophenol, 25 mg of xylene cyanol, and 3 mL of 500 mM EDTA (pH 8.0) were mixed, and 50 mL of DW was used to prepare a 6 × DNA gel loading dye. Moreover, 10 μL of 6X DNA gel loading dye was mixed in the reaction samples. Further, 10 μL of the dye mixture was loaded onto a 1.2 % agarose gel. The gel was electrophoresed at 50 V for 80 min to see the DNA and then photographed with a UV transilluminator. The ability of the samples to protect DNA from damage induced by Fenton's reagent was assessed as follows:

DNA retention (%) = (Intensity of pBluescript SK (+) band in the presence of Fenton's reagent and samples/Intensity of pBluescript SK (+) vector) × 100 (1)

2.9. Statistical and data processing

Data is presented as the mean of pentaplicate measurements (n = 5) ± standard deviation. To establish significant differences, the analysis of variance was performed using the Statistical Analysis System software version 9.4 (SAS Institute, Cary, NC, USA). Tukey's multiple test ($p < 0.05$) was used to confirm the findings. Principal component analysis (PCA) and clustering heatmap analysis were performed using R version 4.3.3 (R Project for Statistical Computing, Vienna, Austria). The PCA biplot, which combined the score and loading plots, was normalized using the "prcomp" function and displayed using the "ggbiplot" package. The heatmap data were normalized using the Z-score, which is given by the following equation:

$$Z\text{-score} = (x - \mu) / \sigma \quad (2)$$

Here, x is the data value, μ is the mean, and σ is the standard deviation.

The clustering was visualized using the Pearson correlation distance measure and Word's clustering method, which were performed using the "pHeatmap" package (Lee et al., 2024b).

3. Results and discussion

3.1. Length and biomass of mung bean plants under the influence of ETL

The effects of ETL treatments on the length of mung bean plants are

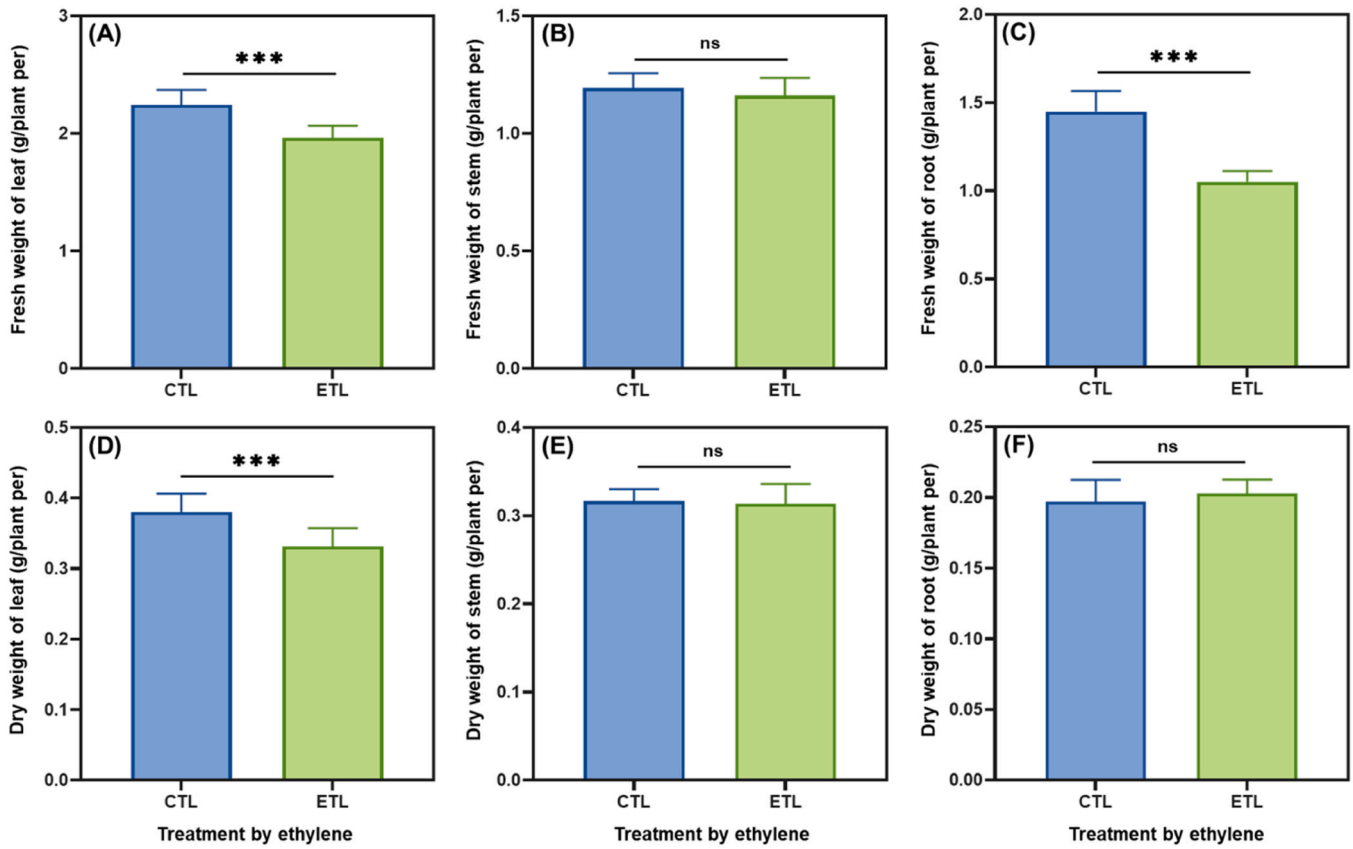

Fig. 3. Biomass amounts of mung bean plant organs by treatment of ethylene. (A) Fresh weight of leaf; (B) Fresh weight of stem; (C) Fresh weight of root; (D) Dry weight of leaf; (E) Dry weight of stem; and (F) Dry weight of root. Abbreviation: CTL, control; ETL, ethylene. All values are expressed as the mean ± standard deviation (n = 10). Significant differences were determined between CTL and ETL by unpaired *t*-test (ns, no significant; *, $p < 0.05$; **, $p < 0.01$; and ***, $p < 0.005$).

presented in Fig. S3. Consequently, the average lengths were 67.50 and 63.99 cm for the CTL and ETL groups, respectively, suggesting that ETL treatments slightly affect plant length. The effects on the biomass are depicted in Fig. 3. Regarding fresh weight, the weight per plant was 2.24 g for leaf-CTL, 1.96 g for leaf-ETL, 1.19 g for stem-CTL, 1.16 g for stem-ETL, 1.45 g for root-CTL, and 1.05 g for root-ETL. Among the organs, the leaves exhibited the highest biomass. Furthermore, the significant difference between ETL treatments showed that leaves and roots, excluding stems, were notably affected. Concerning dry weight, the weight per plant was 0.38 g for leaf-CTL, 0.32 g for leaf-ETL, 0.32 g for stem-CTL, 0.32 g for stem-ETL, 0.21 g for root-CTL, and 0.21 g for root-ETL. This indicates that similar to fresh weight, leaves demonstrated the highest biomass among the organs. Moreover, only leaves exhibited a significant difference.

ETL treatments in plants can influence growth and development through morphological and physiological responses (Dubois et al., 2018). This study indicates that ETL treatments did not significantly alter the overall plant length (Fig. S3). This observation is likely attributed to the short duration of ETL treatments, which did not result in immediate changes in observable growth. Studies indicated that ETL interacts with various phytohormones to regulate cell elongation (Iqbal et al., 2017; Van de Poel et al., 2015); however, prolonged treatment periods are necessary to discern these changes (Yin et al., 2023). Conversely, ETL treatments exhibited a significant effect on biomass, as both the fresh and dry weights of leaves tended to decline (Fig. 3A, D). Thus, ETL functions as a stress hormone, whereby it activates metabolic pathways associated with defense mechanisms rather than promoting growth (Qu et al., 2007). Additionally, ETL has the potential to stimulate senescence-related processes in leaves, resulting in a decrease in chlorophyll content and ultimately leading to reduced leaf biomass (Yu et al., 2021). Furthermore, in the roots, ETL treatment significantly diminished the fresh weight (Fig. 3C). This finding consistently indicates that ETL can regulate root development under stress conditions by inhibiting root elongation and cell division through the suppression of genes implicated in the signaling pathway (Zhou et al., 2024; Vaseva et al., 2018).

3.2. NMR spectroscopic data of the isolated DAE derivatives

Four compounds (**1**–**3** and **9**) were determined by NMR, and their chemical structures were identified as DAE derivatives such as 2′-hydroxydaidzein-4′,7-*O*-diglucoside (**1**, 2HDAEDG), daidzein-4′,7-*O*-diglucoside (**2**, DAEDG), 2′-hydroxydaidzin (**3**, 2HDAI), and 2′-hydroxydaidzein (**9**, 2HDAE) (Fig. 2). Detailed NMR spectra are provided in the Supplementary information (Figs. S4–S7). The NMR spectroscopic data confirmed the substitution patterns of the DAE skeleton with the sugar and hydroxy groups.

Essential data for individual compounds are outlined below: Compound 1 exhibited two distinct anomeric proton signals at δ 4.84 (1 H, H-1″) and 5.12 (1 H, H-1‴) in the ^{1}H NMR spectra, including the presence of two β-glucopyranoside units. The anomeric carbon signals at δ 100.46 (C-1″) and 100.86 (C-1‴) in the ^{13}C NMR data further supported the diglucoside structure. The chemical shifts of C-4′ (δ 158.83) and C-7 (δ 161.85) suggested that the glucoside moieties were attached at these positions. Additionally, the deshielded carbon signal at C-2′ (156.75) with the characteristic ABX aromatic proton patterns confirmed hydroxylation at the 2′ position. Therefore, compound 1 was tentatively assigned as 2HDAEDG (**1**) in comparison with literature data (Kobayashi and Ohta, 1983). The ^{1}H NMR and ^{13}C NMR data of compound 2 revealed structural features similar to compound 1, except that it lacked the 2′-hydroxyl substitution. Two anomeric proton signals at δ 4.90 (1 H, H-1″) and 5.10 (1 H, H-1‴) confirmed diglucosylation. The sugar region showed multiplets in the δ 3.16–3.69, and aromatic signals for the DAE structure appeared at δ 7.08–8.44, including a pair of doublets at δ 7.08 (2 H, d, J = 8.0 Hz, H-3′, 5′) and 7.51 (2 H, d, J = 8.0 Hz, H-2′, 6′), indicative of a parasubstituted B-ring. Characteristic glucose carbon signals were observed between δ 60.66–77.23. The anomeric carbons at δ 99.99 (C-1″) and 110.35 (C-1‴) were consistent with two glucose residues. The absence of a downfield-shifted C-2′ signal, in contrast to compound 1, indicated the lack of a hydroxyl group at this position. This observation supports the structural assignment of DAEDG (**2**), which features diglucosidic substitutions at the C-4′ and C-7 positions of the DAE moiety (Fujitaka et al., 2019). The ^{1}H NMR spectrum of compound 3 exhibited one anomeric proton at δ 5.11 (H-1″), suggesting a single glucosylation, most likely at the 7-position. Furthermore, the glucose signals appeared at δ 2.51–3.72, corresponding to H-2″ to H-6″. The aromatic proton signals confirmed a typical isoflavone skeleton, and signals at δ 6.27 and 6.36 were consistent with an ABX spin system in the B-ring, supporting the presence of a hydroxyl at C-2′. Six glucose carbons (δ 60.66–77.22) and an anomeric carbon (δ 100.02, C-1″) were observed in the ^{13}C NMR spectrum. Additionally, the signal at δ 156.38 supported hydroxylation at C-2′. Overall, these data confirmed the structure as 2′-hydroxydaidzein glucosylated at C-7. This compound was tentatively established as 2HDAI (**3**) of the monoglucoside derivative and was in agreement with the previous literature (Bai et al., 2016). In the ^{1}H NMR and ^{13}C NMR spectra of compound 9, the absence of anomeric proton and sugar signals supported its nonglycosylated aglycone. Moreover, aromatic protons appeared in the range of δ 6.25–8.12, and a distinct ABX pattern (H-3″, H-5″, and H-6″) in the B-ring (δ 6.25, 6.34, 6.84) supported the presence of a 2′-hydroxyl group. All aromatic carbons were present, including a characteristic downfield shift at δ 156.81 (C-2′), indicating hydroxylation. In particular, the carbon signals at δ 154.75 (C-2), 157.88 (C-9), and 158.79 (C-4′) were consistent with the isoflavone skeleton compared to those of the other DAE derivatives **1**–**3**. Based on the above data, compound 9 was elucidated as 2HDAE (**9**) (Bai et al., 2016; Yoo et al., 2004). ^{1}H and ^{13}C NMR spectroscopic data are detailed below.

2HDAEDG (**1**). Amorphous brown powder; EIMS m/z 594; ^{1}H NMR (500 MHz, DMSO-d_6): δ 3.22 (3 H, m, H-2″, H-4″, H-5‴), 3.27 (4 H, m, H-3″, H-2‴, H-3‴, H-4‴), 3.48 (3 H, m, H-5″, H-6α‴, H-6β‴), 3.72 (2 H, m, H-6α″, H-6β″), 4.57 (OH, t, J = 8.0, 4.0 Hz, H-6″), 4.62 (OH, t, J = 8.0, 4.0 Hz, H-6‴), 4.84 (1 H, d, J = 4.0 Hz, H-1″), 5.02 (OH, d, J = 4.0 Hz, H-4″), 5.10 (2OH, d, J = 4.0 Hz, H-2″, H-2‴), 5.12 (1 H, d, J = 4.0 Hz, H-1‴), 5.16 (OH, d, J = 4.0 Hz, H-4‴), 5.33 (OH, d, J = 4.0 Hz, H-3″), 5.46 (OH, d, J = 4.0 Hz, H-3‴), 6.56 (1 H, dd, J = 8.0, 4.0 Hz, H-5′), 6.59 (1 H, d, J = 4.0 Hz, H-3′), 7.11 (1 H, d, J = 4.0 Hz, H-6′), 7.15 (1 H, dd, J = 8.0, 4.0 Hz, H-6), 7.25 (1 H, d, J = 4.0 Hz, H-8), 8.03 (1 H, d, J = 4.0 Hz, H-5), and 8.27 (1 H, s, H-2). ^{13}C NMR (125 MHz, DMSO-d_6): δ 61.05 (C-6″), 61.12 (C-6‴), 70.05 (C-4″), 70.11 (C-4‴), 73.61 (C-2″), 73.68 (C-2‴), 76.94 (C-3″), 77.09 (C-3‴), 77.48 (C-5″), 77.67 (C-5‴), 100.46 (C-1″), 100.86 (C-1‴), 103.91 (C-8), 104.49 (C-3′), 107.19 (C-5′), 113.31 (C-1′), 116.03 (C-6), 118.90 (C-10), δ 122.23 (C-3), 127.34 (C-5), 132.55 (C-6′), 155.36 (C-2), 156.75 (C-2′), 157.57 (C-9), 158.83 (C-4′), 161.85 (C-7), and 175.38 (C-4).

DAEDG (**2**). Amorphous brown powder; EIMS m/z 578; ^{1}H NMR (500 MHz, DMSO-d_6): δ 3.16 (1 H, m, H-4″), 3.27 (5 H, m, H-2″, 3″, 4‴, 5‴), 3.46 (4 H, m, H-2‴, 3‴, 6‴, 5″), 3.69 (1 H, m, H-6″), 4.90 (1 H, d, J = 4.0 Hz, H-1″), 5.10 (1 H, d, J = 4.0 Hz, H-1‴), 7.08 (2 H, d, J = 8.0 Hz, H-3′, 5′), 7.14 (1 H, dd, J = 8.0, 4.0 Hz, H-6), 7.23 (1 H, d, J = 4.0 Hz, H-8), 7.51 (2 H, d, J = 8.0 Hz, H-2′, 6′), 8.04 (1 H, d, J = 4.0 Hz, H-5), and 8.44 (1 H, s, H-2). ^{13}C NMR (125 MHz, DMSO-d_6): δ 60.66 (C-6″), 60.71 (C-6‴), 69.65 (C-4″), 69.73 (C-4‴), 73.16 (C-2″), 73.27 (C-2‴), 76.50 (C-3″), 76.65 (C-3‴), 77.07 (C-5″), 77.23 (C-5‴), 99.99 (C-1″), 110.35 (C-1‴), 103.45 (C-8), 115.70 (C-6), 116.00 (C-3′, 5′), 118.47 (C-10), 123.36 (C-3), 125.30 (C-1′), 127.01 (C-5), 130.01 (C-2′, 6′), 153.85 (C-2), 157.09 (C-4′), 157.19 (C-9), 161.49 (C-7), and 174.67 (C-4).

2HDAI (**3**). Amorphous brown powder; EIMS m/z 432; ^{1}H NMR (500 MHz, DMSO-d_6): δ 2.51 (1 H, m, H-4″), 3.33 (2 H, m, H-2″, H-3″), 3.47 (2 H, m, H-5″, H-6α″), 3.72 (1 H, dd, J = 8.0, 4.0 Hz, H-6β″), 5.11 (1 H, s, H-1″), 6.27 (1 H, dd, J = 8.0, 4.0 Hz, H-5′), 6.36 (1 H, d, J = 8.0 Hz, H-3′), 6.99 (1 H, d, J = 8.0 Hz, H-6′), 7.14 (1 H, dd, J = 8.0, 4.0 Hz, H-6), 7.23 (1 H, d, J = 4.0 Hz, H-8), 8.01 (1 H, d, J = 8.0 Hz, H-

5), and 8.23 (1 H, s, H-2). ^{13}C NMR (125 MHz, DMSO-d_6): δ 60.66 (C-6″), 69.66 (C-4″), 73.16 (C-2″), 76.49 (C-3″), 77.22 (C-5″), 100.02 (C-1″), 102.81 (C-3′), 103.40 (C-8), 106.27 (C-5′), 109.88 (C-1′), 115.50 (C-6), 118.46 (C-10), 122.05 (C-3), 126.88 (C-5), 132.14 (C-6′), 154.77 (C-2), 156.38 (C-2′), 157.06 (C-9), 158.44 (C-4′), 161.34 (C-7), and 175.10 (C-4).

2HDAE (**9**). Amorphous brown powder; EIMS *m/z* 270; ^{1}H NMR (500 MHz, DMSO-d_6): δ 6.25 (1 H, dd, *J* = 8.0, 4.0 Hz, H-5′), 6.34 (1 H, d, *J* = 4.0 Hz, H-3′), 6.84 (1 H, d, *J* = 4.0 Hz, H-6′), 6.91 (1 H, dd, *J* = 8.0, 4.0 Hz, H-6), 6.95 (1 H, d, *J* = 8.0 Hz, H-8), 7.92 (1 H, d, *J* = 12.0 Hz, H-5), and 8.12 (1 H, s, H-2). ^{13}C NMR (125 MHz, DMSO-d_6): δ 102.49 (C-8), 103.28 (C-3′), 106.71 (C-5′), 110.57 (C-1′), 115.51 (C-6), 116.98 (C-10), 122.23 (C-3), 127.64 (C-5), 132.53 (C-6′), 154.75 (C-2), 156.81 (C-2′), 157.88 (C-9), 158.79 (C-4′), 162.91 (C-7), and 175.60 (C-4).

Overall, the ^{1}H and ^{13}C NMR spectral data confirmed that 2HDAEDG, DAEDG, and 2HDAI possess glycosyl moieties associated with the 4′ or 7 positions of the DAE core. 2HDAEDG, 2HDAI, and 2HDAE represent forms with additional hydroxyl substitutions (Fujitaka et al., 2019; Bai et al., 2016; Yoo et al., 2004; Kobayashi and Ohta, 1983). This observation highlights the diversity of isoflavone compounds found in mung bean leaves, suggesting that these compounds may play a significant role in the biological activity (Ganesan and Xu, 2017).). In this study, the structural elucidation of HDAI and HDAE yielded results consistent with those previously reported for mung bean leaves (Bai et al., 2016). This facilitated the reconfirmation of the existence and characteristics of these isoflavones in mung bean leaves.

3.3. Quantification of bioactive metabolites

Ten isoflavone and three flavone derivatives were identified as the main bioactive metabolites in mung bean organs. Their typical HPLC chromatogram and chemical structures are shown in Fig. 2, providing a quantitative basis for evaluating metabolite changes across different organs and treatment conditions. The typical HPLC chromatograms of isoflavones and flavones from mung bean organs under ETL treatment are presented in Fig. 4, and their quantified contents are presented in Table 1, Fig. 5A, and B. The total isoflavone contents exhibited a 31.1-fold increase, rising from SD (7.77 μg/g) to GM (241.70 μg/g). At 28 days of growth, the total isoflavone contents in leaf-, stem-, and root-CTL were approximately 1119.46, 965.68, and 27,067.06 μg/g, respectively. In fact, ETL treatment significantly increased these contents to 66,999.28 μg/g for leaf-ETL, 17,745.41 μg/g for stem-ETL, and 41,272.63 μg/g for root-ETL (Table 1). Notably, total isoflavone contents in leaf-ETL increased 59.8-fold compared to leaf-CTL, identifying the leaf as the main organ for isoflavone accumulation (Fig. 5A). Among individual isoflavone derivatives, 2HDAI (**3**), DAI (**4**), and GEI (**8**) showed the most pronounced increases, rising from 273.24 to 21,159.88 μg/g (77.4-fold), from 429.67 to 31,845.13 μg/g (74.2-fold), and from 268.35 to 3209.12 μg/g (12.0-fold) of the leaves. Although these derivatives were predominantly abundant in leaf-ETL, diglycoside isoflavones exhibited the highest accumulation in root-ETL. In contrast to isoflavones, the total flavone content decreased from SD (4797.63 μg/g) to GM (2058.17 μg/g). However, the total flavone contents increased within the mung bean organs after 28 days of sowing and significantly increased after ETL treatment. In particular, the flavone contents in leaf-, stem-, and root-CTL were approximately 34,785.02, 3171.11, and 10,896.63 μg/g, respectively, whereas ETL treatment increased these contents to 47,606.19 μg/g for leaf-ETL, 9535.17 μg/g for stem-ETL, and 22,558.18 μg/g for root-ETL (Table 1). The ETL treated leaves exhibited significantly higher flavone contents than the other organs, further supporting the leaf as the main organ of flavone accumulation (Fig. 5B). Among the individual flavone derivatives, IVTX (**7**) showed the highest accumulation in leaves, increasing approximately 1.3-fold

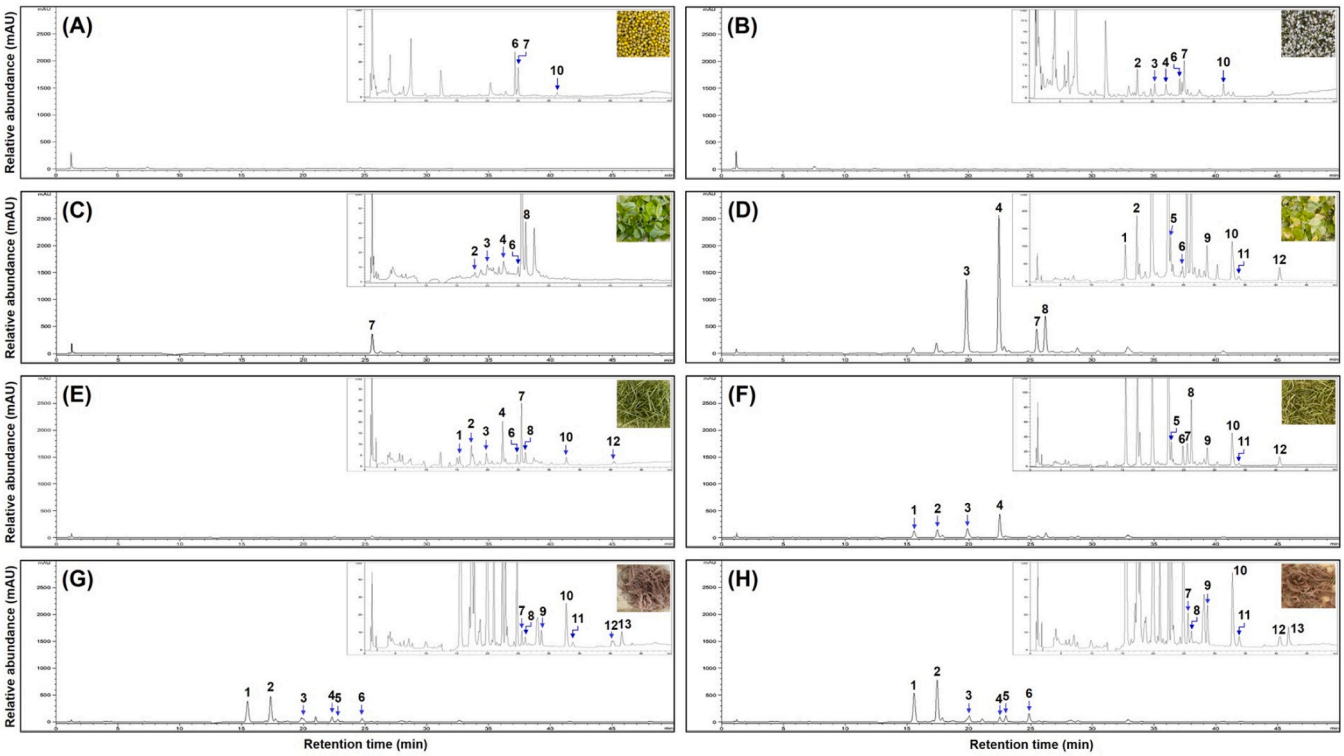

Fig. 4. Typical HPLC chromatogram of isoflavone and flavone derivatives in 50 % MeOH extracts with mung bean plant organs by treatment with ethylene. Organs of mung bean plant: (A) Seed; (B) germination; (C) leaf-CTL, ethylene treated leaf; (D) leaf-ETL, ethylene treated leaf; (E) stem-CTL, ethylene not-treated stem; (F) stem-ETL, ethylene treated stem; (G) root-CTL, ethylene not-treated root; and (H) root-ETL, ethylene treated root. 13 Chemicals: 1, 2′-hydroxydaidzein-4′,7-*O*-diglucoside (2HDAEDG); 2, daidzein-4′,7-O-diglucoside (DAEDG); 3, 2′-hydroxydaidzin (2HDAI); 4, daidzin (DAI); 5, glycitin (GLI); 6, vitexin (VTX); 7, isovitexin (IVTX); 8, genistin (GEI); 9, 2′-hydroxydaidzein (2HDAE); 10, daidzein (DAE); 11, glycitein (GLE); 12, genistein (GEE); and 13, apigenin (AGN).

Table 1
Comparison of the isoflavone and flavone contents in 50 % MeOH extracts with mung bean plant organs by treatment with ethylene.

Contents[a] (μg/g)	Organs of mung bean plant							
	SD	GM	Leaf		Stem		Root	
			CTL	ETL	CTL	ETL	CTL	ETL
Isoflavone derivatives								
Diglycosides								
2HDAEDG (**1**)	nd[b]	nd	nd	3500.80 ± 68.45 d	149.59 ± 25.51 e	4687.14 ± 109.74 c	13,863.01 ± 90.86 b	19,261.68 ± 100.06 a
DAEDG (**2**)	nd	140.76 ± 10.76 f	148.21 ± 10.75 f	3963.15 ± 1.26 c	309.72 ± 6.70 e	3169.63 ± 5.65 d	9948.68 ± 9.89 b	16,694.68 ± 11.16 a
Total	0	140.76	148.21	7463.95	459.30	7856.78	23,811.69	35,956.36
Glycosides								
2HDAI (3)	nd	39.41 ± 1.28 g	273.24 ± 6.91 e	21,159.88 ± 16.15 a	119.84 ± 7.26 f	2952.38 ± 0.52 b	1115.94 ± 10.07 d	2372.57 ± 0.84 c
DAI (**4**)	nd	47.74 ± 4.37 e	429.67 ± 15.95 d	31,845.13 ± 154.53 a	259.99 ± 0.23 de	5509.80 ± 2.59 b	1139.42 ± 2.03 c	1142.37 ± 0.79 c
GLI (**5**)	nd	nd	nd	971.46 ± 1.14 a	nd	261.40 ± 0.41 d	356.17 ± 0.54 c	820.70 ± 0.23 b
GEI (**8**)	nd	nd	268.35 ± 12.98 c	3209.12 ± 3.87 a	103.67 ± 1.21 e	495.67 ± 0.51 b	115.80 ± 1.06 de	131.36 ± 0.16 d
Total	0	87.15	971.25	57,185.59	483.51	9219.26	2727.32	4467.01
Aglycones								
2HDAE (**9**)	nd	nd	nd	768.14 ± 0.95 a	nd	167.52 ± 1.71 d	237.53 ± 3.45 c	354.37 ± 2.98 b
DAE (**10**)	7.77 ± 0.47 g	13.79 ± 1.52 f	nd	1136.00 ± 1.83 a	22.87 ± 0.30 e	379.64 ± 1.42 b	201.38 ± 1.73 d	355.40 ± 0.45 c
GLE (**11**)	nd	nd	nd	230.98 ± 5.99 a	nd	56.89 ± 0.82 c	65.06 ± 2.28 c	104.20 ± 1.29 b
GEE (**12**)	nd	nd	nd	214.63 ± 1.29 a	nd	65.32 ± 0.47 b	24.09 ± 3.33 c	35.29 ± 3.39 d
Total	7.77	13.79	0	2349.74	22.87	669.38	528.05	849.26
Total isoflavones	**7.77**	**241.70**	**1119.46**	**66,999.28**	**965.68**	**17,745.41**	**27,067.06**	**41,272.63**
Flavone derivatives								
VTX (**6**)	2014.26 ± 23.64 d	270.52 ± 10.01 h	652.25 ± 29.67 f	1932.80 ± 9.73 e	428.60 ± 4.81 g	2598.82 ± 4.99 c	6830.54 ± 6.50 b	15,786.75 ± 20.93 a
IVTX (**7**)	2783.37 ± 68.51 de	1787.65 ± 40.67 e	34,132.77 ± 1508.74 b	45,673.39 ± 56.54 a	2742.51 ± 27.60 de	6936.35 ± 40.01 c	2146.67 ± 54.10 de	4212.96 ± 5.83 d
AGN (**13**)	nd	nd	nd	nd	nd	nd	1919.42 ± 49.07 b	2558.46 ± 20.26 a
Total flavones	**4797.63**	**2058.17**	**34,785.02**	**47,606.19**	**3171.11**	**9535.17**	**10,896.63**	**22,558.18**

*Abbreviation: SD, seed; GM, germination; CTL, control (not-treated ethylene); and ETL, ethylene (treated ethylene). 2HDAEDG, 2′-hydroxydaidzein-4′,7-*O*-diglucoside; DAEDG, daidzein-4′,7-*O*-diglucoside; 2HDAI, 2′-hydroxydaidzin; DAI, daidzin; GLI, glycitin; GEI, genistin; 2HDAE, 2′-hydroxydaidzein; DAE, daidzein; GLE, glycitein; GEE, genistein; VTX, vitexin; IVTX, isovitexin; and AGN, apigenin.

[a] All values are expressed as the mean ± standard deviation of pentaplicate determination. Different small letters correspond to significant differences related to the same row, as determined by the ANOVA and followed by Tukey's multiple tests ($p < 0.05$).

[b] nd: not detected.

from 34,132.77 to 45,673.39 μg/g. In contrast, VTX (**6**) and AGN (**13**) were primarily accumulated in roots, with VTX (**6**) levels rising 2.3-fold from 6830.54 to 15,786.75 μg/g and AGN (**13**) increasing 1.3-fold from 1919.42 to 2558.46 μg/g (Table 1).

PCA biplot and heatmap clustering were employed to elucidate the variances in the bioactive metabolite profiles associated with the mung bean organs following ETL treatment (Fig. 6). The PCA results indicated that PC1 and PC2 accounted for 62.21 % and 34.01 % of the total variance, respectively. The score plot effectively illustrated significant differences among mung bean organs based on various treatment conditions, as evidenced by the discernible separation of data points (Fig. 6A). Similarly, the heatmap analysis corroborated the PCA findings, revealing distinct variations in isoflavone and flavone derivatives between treated and untreated organs with respect to ETL (Fig. 6B). The loading plot further identified the key metabolites contributing to these observed differences. Specifically, 2HDAEDG (**1**), DAEDG (**2**), VTX (**6**), and AGN (**13**) exhibited strong associations with the root-ETL, whereas 2HDAI (**3**), DAI (**4**), IVTX (**7**), GEI (**8**), 2HDAE (**9**), DAE (**10**), GLE (**11**), and GEE (**12**) were closely linked to the leaf-ETL (Fig. 6A). These findings were further validated by hierarchical clustering analysis, which categorized the metabolites into two primary clusters: one that was strongly correlated with leaf-ETL and the other with root-ETL (Fig. 6B).

The results for TP and TF contents are presented in Fig. 5C and D. Data revealed that leaf-ETL exhibited the highest TP and TF contents at approximately 24.59 and 12.87 mg/g, respectively. Additionally, leaf-CTL had the second-highest levels, with TP and TF contents of 13.87 and 9.89 mg/g, respectively. No significant difference was observed in TP contents among the other mung bean organs. Likewise, TF contents showed significant differences in other organs, except for GM. These results highlight the influence of ETL treatment on the accumulation patterns of bioactive metabolites in mung bean plant organs.

Alterations in plant metabolites are widely recognized for their critical bioactivities pertaining to growth, regulatory functions, and defense mechanisms (Tripathi et al., 2024; Selwal et al., 2023). This study examined the variations in isoflavones and flavones in mung bean plants following ETL treatment. The concentration of isoflavones increased, whereas the concentration of flavones decreased during germination (Table 1). This observation aligns with the results of a previous study indicating that isoflavones increased and flavones decreased during the transition from SD to GM, wherein isoflavone biosynthesis was stimulated during germination and flavones exhibited an inhibitory effect on flavone metabolism (Zhang et al., 2022; Lu et al., 2019). ETL treatment led to a notable accumulation of bioactive metabolites in mung bean plants (Fig. 6). Similarly, although treatments with plant signaling molecules (ETL, 1-aminocyclopropane-1-carboxylic acid, and salicylic acid, etc.) are not universally effective across all species, a study demonstrated that they can significantly enhance the accumulation of main metabolites in select plants such as soybeans and *A. acutiloba* (Lee et al., 2024a; Kim et al., 2023; Lee et al., 2023; Kim et al., 2022). Specifically, Kim et al. (2023) and Lee et al. (2023) demonstrated that the application of signaling molecules enhanced the expression of isoflavone biosynthetic genes in soybean leaves and

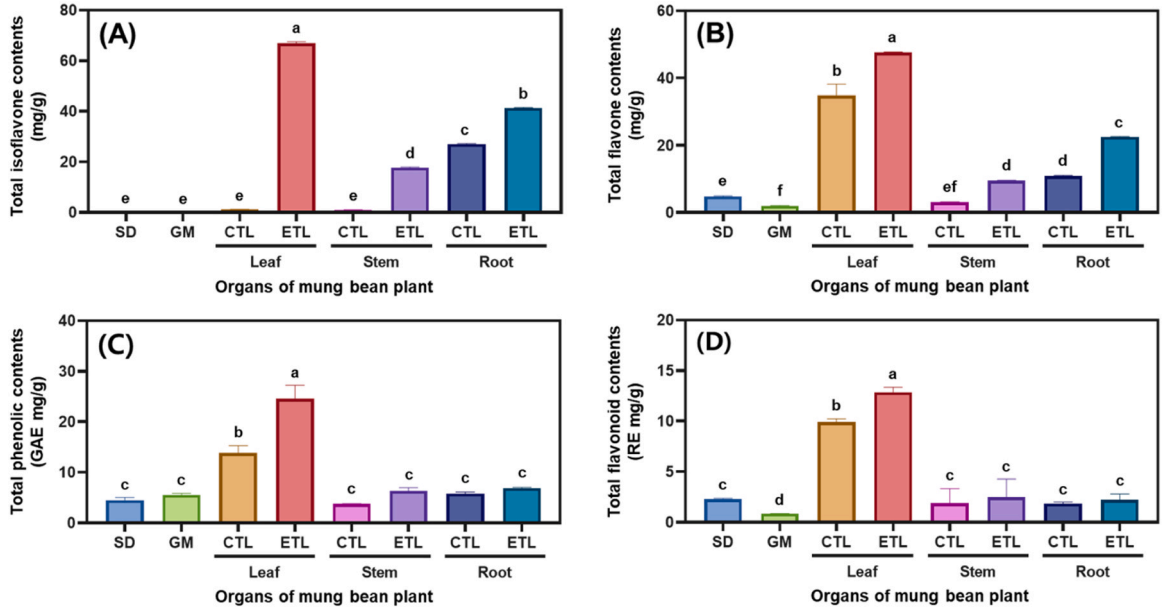

Fig. 5. Total isoflavone and flavone contents for mung bean plant organs by treatment with ethylene. (A) Total isoflavone contents; (B) total flavone contents; (C) Total phenolic contents; and (D) total flavonoid contents. Abbreviation: SD, seed; GM, germination; CTL, control; ETL, ethylene. All values are expressed as the mean ± standard deviation of pentaplicate determination. Different small letters correspond to significant differences related to organs of mung bean plant, as determined by the ANOVA and followed by Tukey's multiple tests ($p < 0.05$).

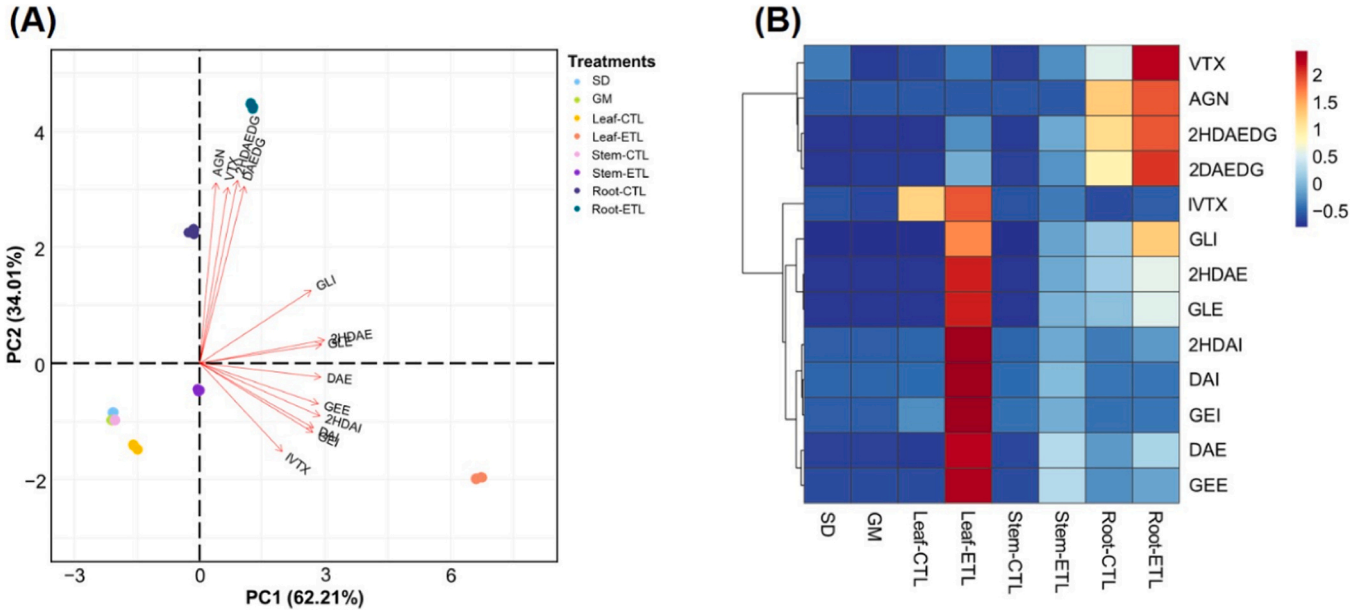

Fig. 6. Visualization of normalized data using Z-score for isoflavone and flavone derivatives in mung bean plant organs by treatment with ethylene. (A) Biplot with principal component analysis (PCA) and (B) heat maps applied with Pearson correlation distance measure and Ward's clustering methods. Abbreviation: SD, seed; GM, germination; leaf-CTL, control leaf; leaf-ETL, ethylene treated leaf; stem-CTL, control stem; stem-ETL, ethylene treated stem; root-CTL, control root; and root-ETL, ethylene treated root. 2HDAEDG, 2′-hydroxydaidzein-4′,7-*O*-diglucoside; DAEDG, daidzein-4′,7-*O*-diglucoside; 2HDAI, 2′-hydroxydaidzin; DAI, daidzin; GLI, glycitin; VTX, vitexin; IVTX, isovitexin; GEI, genistin; 2HDAE, 2′-hydroxydaidzein; DAE, daidzein; GLE, glycitein; GEE, genistein; and AGN, apigenin.

induced the accumulation of malonyl-DAI and malonyl-GEI. Moreover, Kim et al. (2022) revealed that soybean root tissues induce the accumulation of DAE and coumestrol through metabolic pathways distinct from those observed in leaves. Furthermore, Lee et al. (2024a) reported that signaling molecules regulate the accumulation of furanocoumarins in *A. acutiloba* roots, suggesting that root organs may serve as significant sites for the accumulation of specific metabolites. These studies have indicated the potential for a metabolite-enriched plant strategy when the scope of application is broadened to encompass various plants in the future. In this study, specific compounds, namely, 2HDAEDG, 2HDAI, and 2HDAE, which were detected in trace amounts and therefore limited the efficacy evaluation (Bia et al., 2016; Yoo et al., 2004; Kobayashi and Ohta, 1983), were secured in substantial quantities by ETL processing, thereby proposing a new paradigm for both *in vivo* and *in silico* efficacy verification and the discovery of new drug candidates in the future (He et al., 2024; Park et al., 2023; Atanasov et al., 2021).

Finally, a study was previously reported that increased isoflavone contents (six isoflavone derivatives) by treating soybean leaves with

ethylene, a signaling molecule (Ban et al., 2020). However, mung bean leaves grown in a vertical farm for about 30 days and treated with ethylene, ten isoflavone derivatives were produced compared to the seeds, and the amount increased by approximately 59.9-fold (Leaf-CTL: 1119.46 μg/g → Leaf-ETL: 66,999.28 μg/g) compared to untreated leaves. Especially, the malonyl-DAI and malonyl-GEI increased in soybean leaves. However, the and daidzin 2HDAI and DAI increased greatly in mung bean leaves. The results of this study are the first report in the world to be confirmed by our research team.

ETL treatment resulted in significant alterations in TP and TF contents across mung bean plant organs, which were closely associated with the accumulation of bioactive metabolites. Notably, the most pronounced enhancement was observed in the leaves of mung bean plants (Fig. 5C and D). The findings strongly indicate that ETL treatment not only activates organ-specific secondary metabolic pathways but also enhances the stress-responsive capacity of mung bean plants through the modulation of key enzymatic pathways (Gupta et al., 2018a). Notably, the TP and TF accumulation in the leaves emphasizes the role of ETL in amplifying the antioxidant defense mechanisms under abiotic stress conditions (Gupta et al., 2018b; Pisoschi and Pop, 2015). This observation aligns with prior reports that ETL modulates oxidative stress responses by upregulating genes within the phenylpropanoid and flavonoid biosynthesis pathways, thereby contributing to increased cellular resilience (Kim et al., 2023; Yin et al., 2023; Dubois et al., 2018). Consequently, the leaves serve as a primary site for the accumulation of bioactive metabolites. Therefore, the mung bean leaves, enriched with flavones in response to ETL treatment, hold significant potential applications in metabolite farming and development of functional bioresources.

3.4. Influences on in vitro biological activities

The antioxidant abilities were evaluated through the DPPH and ABTS radical scavenging activities, and the corresponding IC_{50} values are displayed in Fig. 7A and B. In the DPPH radical scavenging activity, the SD and GM values were relatively high at 5.91 and 5.83 mg/mL, respectively, showing no significant difference. The IC_{50} values in various organs of mung bean plants were ranked as stems > roots > leaves, with leaves exhibiting the lowest value. Specifically, the values were 0.76 mg/mL for leaf-CTL and 0.32 mg/mL for leaf-ETL. The ABTS radical scavenging activity revealed lower IC_{50} values than the DPPH radical scavenging activity. Additionally, SD and GM demonstrated lower IC_{50} values than those observed in the stems and roots. Notably, similar lowest values were recorded in leaves, specifically 0.17 mg/mL for CTL-leaf and 0.09 mg/mL for ETL-leaf. The digestive enzyme-inhibition abilities were assessed through α-glucosidase and pancreatic lipase-inhibition activities, and the relevant IC_{50} values are shown in Fig. 7C and D. The α-glucosidase-inhibition activity was most pronounced in mung bean roots, particularly at 7.38 mg/mL for root-CTL and 3.20 mg/mL for root-ETL. Meanwhile, leaf-ETL exhibited an activity of 6.41 mg/mL, with no significant difference compared with the root. Regarding pancreatic lipase-inhibition activity, before treatment, leaf-CTL exhibited 23.77 mg/mL and root-CTL exhibited 21.74 mg/mL, showing similar levels. Following ETL treatment, leaf-ETL measured 9.73 mg/mL and root-ETL measured 17.78 mg/mL. Thus, ETL treatment may reduce the IC_{50} values, with the most effective activities observed in the leaves.

Antioxidant activity is important in human health through free radical scavenging, oxidative stress reduction, and metal ion-chelating ability (Kim, 2021; Csire et al., 2020). The DPPH and ABTS radical scavenging activities are commonly used to assess this antioxidant activity (Wójciak et al., 2024). Moreover, α-glucosidase and pancreatic lipase-inhibition activities are important in digestion, contributing to the regulation of blood glucose levels and anti-obesity effects (Barańska et al., 2021; Choi et al., 2010). These antioxidant- and enzyme-inhibition activities are closely correlated with the contents of polyphenol compounds, including isoflavones and flavonoids (Lee et al., 2024c; Kim et al., 2023; Hwang et al., 2021; Ban et al., 2020). In this study, leaves exhibited the lowest IC_{50} values among mung bean organs (Fig. 7), suggesting that the leaves have the highest antioxidant- and digestive enzyme-inhibition activities. Notably, leaves consistently demonstrated the highest antioxidant- and digestive enzyme-inhibition activities (Kim et al., 2020; Sathasivam et al., 2025). This improvement in the *in vitro* biological activity following ETL treatment is likely due to the metabolic plasticity changes induced by ETL signaling (Tripathi et al., 2024; Kim et al., 2023). This finding means that ETL treatment can activate secondary metabolic pathways to increase the synthesis of flavonoids, phenolics, and other antioxidant compounds

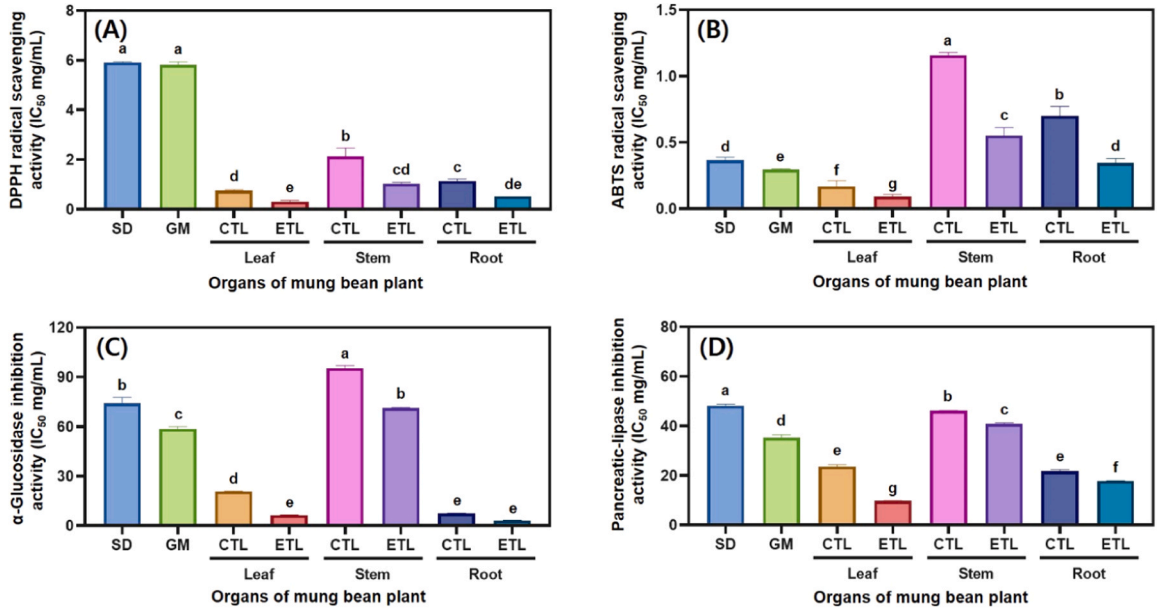

Fig. 7. Comparison of IC_{50} values of *in vitro* biological activities for 50 % MeOH extracts with mung bean plant organs by treatment with ethylene. (A) DPPH radical scavenging activity; (B) ABTS radical scavenging activity; (C) α-glucosidase inhibition activity; and (D) pancreatic-lipase inhibition activity. Abbreviation: SD, seed; GM, germination; CTL, control (untreated ethylene); and ETL, ethylene (treated ethylene).

(Lee et al., 2024a; Lee et al., 2023). This demonstrated the important role of ETL treatments in improving plant physiological activity by regulating metabolic pathways related to defense responses (Tripathi et al., 2024; Gupta et al., 2018b; Pisoschi and Pop, 2015). The present findings are consistent with those of previous studies, which demonstrated that an increase in the isoflavone content enhances the antioxidant- and digestive enzyme-inhibition activities (Lee et al., 2023). Meanwhile, the roots exhibited high α-glucosidase-inhibition activity, which was likely correlated with the high diglycoside isoflavone contents in the roots (Fig. 7D). Studies have reported that isoflavones have α-glucosidase-inhibition activity and excellent blood sugar control and antidiabetic effects (Barańska et al., 2021; Choi et al., 2010). However, to date, there has been little research on whether diglycoside isoflavones directly exhibit α-glucosidase inhibitory activity, and this discovery presents a new frontier in enzyme inhibitory activity.

3.5. Influence on oxidative DNA damage protection

To evaluate the effect of ETL treatment on the *in vitro* bioactivity of mung bean organs, the oxidative protection effect of the mung bean extracts was analyzed. For this purpose, each sample extract was diluted to 100, 50, and 25 μg/mL to compare the DNA protection (Figs. S8–S10). After setting the concentration at 50 μg/mL, the influence on the oxidative DNA damage protection of each sample was analyzed (Fig. 8). The SC bands were observed at 10.55 % for SD and 26.60 % for GM. In other mung bean organ comparisons, SC ratios were 95.68 % for leaf-CTL, 90.05 % for leaf-ETL, 3.89 % for stem-CTL, 56.14 % for stem-ETL, 60.88 % for root-CTL, and 76.37 % for root-ETL samples. A slight but no significant decrease was noted after ETL treatment in the leaves, whereas the stems and roots showed a significant increase. These results may provide important evidence for the differential organs specific bioactivity of ETL treatment.

DNA exhibits significant vulnerability to ROS-induced oxidative damage, which may result in strand breaks, base modifications, and transformation of the SC form into open circular DNA (OC) or linear DNA (LIN) forms (Chatterjee and Walker, 2017). Such oxidative damage arises from a multitude of environmental stressors, UV radiation, pollutants, and metabolic byproducts, thereby underscoring the need for robust mechanisms to protect DNA (Juan et al., 2021). Numerous studies have emphasized the substantial role of bioactive metabolites in scavenging ROS and safeguarding DNA (Khole et al., 2016; Xiao et al., 2016). This study demonstrated the most pronounced protective effect on DNA resulting from the application of extracts from mung bean leaves, correlating with their significant accumulation of these bioactive metabolites. Furthermore, ETL application to mung bean stems and roots appeared to enhance the DNA-protective effect (Fig. 8). This observation substantiates the established notion that high levels of antioxidants within plant tissues are intricately associated with improved DNA protection and diminished ROS levels (Lee et al., 2024b; Kalim et al., 2010). Isoflavones and flavones are flavonoid compounds that have DNA protection, and the mechanisms through which they scavenge ROS and chelate metal ions relevant to radical formation empower them to effectively mitigate oxidative damage (Khole et al., 2016; Xiao et al., 2016). Agricultural practices incorporating ETL treatment present a promising avenue for enhancing the production of bioactive metabolites and subsequently advancing DNA protection.

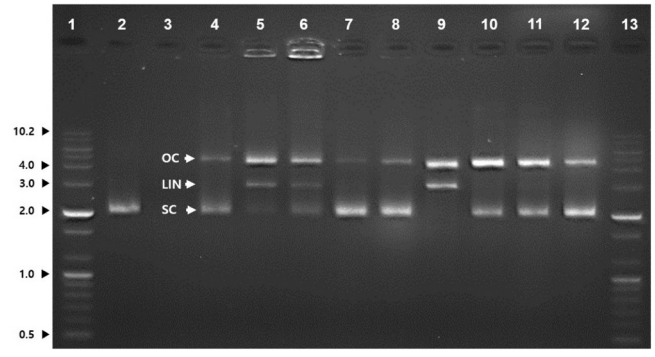

Fig. 8. DNA-protection of 50 % MeOH extracts with mung bean plant organs by treatment with ethylene. Lane 1 & 13, size mark; lane 2, pBluescript SK(+); lane 3, 50 % MeOH; lane 4, pBluescript SK(+) + fenton's reagent (H_2O_2); lane 5–12, pBluescript SK(+) + H_2O_2 + samples (lane5, SD; lane 6, GM; lane 7, leaf-CTL; lane 8, leaf-ETL; lane 9, stem-CTL; lane 10, stem-ETL; lane 11, root-ETL; lane 12, root-ETL). Abbreviations: SD, seed; GM, germination; CTL, control (not treated with ethylene); ETL, ethylene treated; OC, open circular DNA; LIN, linear DNA; SC, supercoiled DNA.

4. Conclusions

The results of this study indicate that ETL treatment significantly influences the metabolites in mung bean plants, consequently upscaling the production of novel bioactive compounds belonging to the flavonoid family. Notably, the accumulation of bioactive metabolites (isoflavones and flavones) is increased in ETL treated mung bean plants. Specifically, while SD, GM, and CTL exhibited minimal bioactive metabolites, a substantial increase in isoflavones (from 1119.46 to 66,999.28 μg/g, 59.9-fold) and flavones (from 34,785.02 to 47,606.19 μg/g, 1.4-fold) were observed in the ETL treated leaves. Moreover, the TP and TF contents were significantly increased. These metabolite alterations demonstrate a robust correlation with the *in vitro* biological and DNA protection activities. This finding implies the potential for regulating specific functional components, thereby introducing a novel paradigm for the development of functional bioresources utilizing agricultural residues. Furthermore, although this study illustrates ETL as a potent inducer for the production of bioactive metabolites in legumes and as a stress-responsive signaling molecule, more studies into the gene expression within the isoflavonoid biosynthesis pathway are essential to elucidate the mechanisms driving these changes. Future studies may elucidate the regulatory network and enzyme activities involved in ETL-induced isoflavonoid biosynthesis. Successful elucidation of these gene regulation mechanisms would provide scientific validation for the advancement of the next generation of dietary supplements and nutraceuticals based on functional bioresources.

CRediT authorship contribution statement

Jong Bin Jeong: Investigation, Formal analysis. **Hee Yul Lee:** Validation, Investigation. **Eun Jeong Ko:** Investigation, Formal analysis. **Du Yong Cho:** Writing – original draft, Visualization, Methodology, Conceptualization. **Kye Man Cho:** Writing – review & editing, Supervision, Resources, Project administration, Conceptualization. **Mu Yeun Jang:** Software, Formal analysis. **Se Hyeon Jeon:** Visualization, Software, Data curation. **Ki-Ho Son:** Validation, Methodology. **Ga Yong Lee:** Formal analysis, Data curation. **Jin Hwan Lee:** Writing – review & editing, Writing – original draft, Resources, Methodology, Funding acquisition, Conceptualization. **Md. Azizul Haque:** Writing – review & editing, Writing – original draft.

Funding

This work was supported by the Basic Science Research Program through the National Research Foundation (NRF) funded by the Ministry of Education (Grant number RS-2023-00245096) and Ministry of Science and ICT (RS-2024-00346785), Republic of Korea.

Declaration of Competing Interest

The authors declare that they have no known competing financial interests or personal relationships that could have appeared to influence the work reported in this paper.

Appendix A. Supporting information

Supplementary data associated with this article can be found in the online version at doi:10.1016/j.indcrop.2025.121382.

Data availability

Data will be made available on request.

References

Atanasov, A.G., Zotchev, S.B., Dirsch, V.M., et al., 2021. Natural products in drug discovery: advances and opportunities. Nat. Rev. Drug Discov. 20, 200–216. https://doi.org/10.1038/s41573-020-00114-z.

Bai, Y., Xu, Y., Chang, J., Wang, X., Zhao, Y., Yu, Z., 2016. Bioactives from stems and leaves of mung beans (*Vigna radiata* L.). J. Funct. Foods 25, 314. https://doi.org/10.1016/j.jff.2016.06.009.

Bai, Y., Zhang, Q., Wang, B., Zhang, M., Xu, Y., Li, S., Zhao, Y., Yu, Z., 2017. Plasma pharmacokinetics, bioavailability, and tissue distribution of four C-glycosyl flavones from mung bean (*Vigna radiata* L.) seed extracts in rat by ultrahigh-performance liquid chromatography–tandem mass spectrometry. J. Agric. Food Chem. 65 (27), 5570. https://doi.org/10.1021/acs.jafc.7b02053.

Ban, Y.J., Song, Y.H., Kim, J.Y., Baiseitova, A., Lee, K.W., Kim, K.D., Park, K.H., 2020. Comparative investigation on metabolites changes in soybean leaves by ethylene and activation of collagen synthesis. Ind. Crop Prod. 154, 112743. https://doi.org/10.1016/j.indcrop.2020.112743.

Ban, Y.J., Song, Y.H., Kim, J.Y., Cha, J.Y., Ali, I., Baiseitova, A., Shah, A.B., Kim, W., Park, K.H., 2021. A Significant change in free amino acids of soybean (*Glycine max* L. Merr) through ethylene application. Molecules 26 (4). https://doi.org/10.3390/molecules26041128.

Banwo, K., Olojede, A.O., Adesulu-Dahunsi, A.T., Verma, D.K., Thakur, M., Tripathy, S., Singh, S., Patel, A.R., Gupta, A.K., Aguilar, C.N., Utama, G.L., 2021. Functional importance of bioactive compounds of foods with potential health benefits: a review on recent trends. Food Biosci. 43. https://doi.org/10.1016/j.fbio.2021.101320.

Barańska, A., Błaszczuk, A., Polz-Dacewicz, M., Kanadys, W., Malm, M., Janiszewska, M., Jędrych, M., 2021. Effects of soy isoflavones on glycemic control and lipid profile in patients with type 2 diabetes: a systematic review and meta-analysis of randomized controlled trials. Nutrients 13 (6). https://doi.org/10.3390/nu13061886.

Chagas, M.D.S.S., Behrens, M.D., Moragas-Tellis, C.J., Penedo, G.X.M., Silva, A.R., Gonçalves-De-Albuquerque, C.F., 2022. Flavonols and flavones as potential anti-inflammatory, antioxidant, and antibacterial compounds. Oxid. Med. Cell. Longev. 1, 9966750. https://doi.org/10.1155/2022/9966750.

Chatterjee, N., Walker, G.C., 2017. Mechanisms of DNA damage, repair, and mutagenesis. Environ. Mol. Mutagen 58 (5), 235. https://doi.org/10.1002/em.22087.

Choi, C.W., Choi, Y.H., Cha, M., Yoo, D.S., Kim, Y.S., Yon, G.H., Hong, K.S., Kim, Y.H., Ryu, S.Y., 2010. Yeast α-glucosidase inhibition by isoflavones from plants of leguminosae as an in vitro alternative to acarbose. J. Agric. Food Chem. 58 (18), 9988. https://doi.org/10.1021/jf101926j.

Csire, G., Canabady-Rochelle, L., Averlant-Petit, M., Selmeczi, K., Stefan, L., 2020. Both metal-chelating and free radical-scavenging synthetic pentapeptides as efficient inhibitors of reactive oxygen species generation. Metallomics 12 (8), 1220. https://doi.org/10.1039/d0mt00103a.

Dubois, M., Van Den Broeck, L., Inzé, D., 2018. The pivotal role of ethylene in plant growth. Trends Plant Sci. 23 (4), 311. https://doi.org/10.1016/j.tplants.2018.01.003.

Fujitaka, Y., Hamada, H., Uesugi, D., Kuboki, A., Shimoda, K., Iwaki, T., Kiriake, Y., Saikawa, T., 2019. Synthesis of daidzein glycosides, α-tocopherol glycosides, hesperetin glycosides by bioconversion and their potential for anti-allergic functional-foods and cosmetics. Molecules 24 (16), 2975. https://doi.org/10.3390/molecules24162975.

Ganesan, K., Xu, B., 2017. A critical review on phytochemical profile and health promoting effects of mung bean (*Vigna radiata*). Food Sci. Hum. Wellness 7 (1), 11. https://doi.org/10.1016/j.fshw.2017.11.002.

Gupta, R., Min, C.W., Kramer, K., Agrawal, G.K., Rakwal, R., Park, K., Wang, Y., Finkemeier, I., Kim, S.T., 2018b. A multi-omics analysis of *Glycine max* leaves reveals alteration in flavonoid and isoflavonoid metabolism upon ethylene and abscisic acid treatment. Proteomics 18 (7). https://doi.org/10.1002/pmic.201700366.

Gupta, R., Min, C.W., Meng, Q., Agrawal, G.K., Rakwal, R., Kim, S.T., 2018a. Comparative phosphoproteome analysis upon ethylene and abscisic acid treatment in *Glycine max* leaves. Plant Physiol. Biochem. 130, 173. https://doi.org/10.1016/j.plaphy.2018.07.002.

Ha, T.J., Park, E.J., Lee, K.S., Seo, W.D., Song, S.B., Lee, M.H., Kim, S., Oh, E., Pae, S.B., Kwak, D.Y., Lee, J.H., 2021. Identification of anthocyanin compositions in black seed coated Korean adzuki bean (*Vigna angularis*) by NMR and UPLC-Q-Orbitrap-MS/MS and screening for their antioxidant properties using different solvent systems. Food Chem. 346, 128882. https://doi.org/10.1016/j.foodchem.2020.128882.

He, D., Liu, Q., Mi, Y., Meng, Q., Xu, L., Hou, C., Wang, J., Li, N., Liu, Y., Chai, H., Yang, Y., Liu, J., Wang, L., Hou, Y., 2024. De novo generation and identification of novel compounds with drug efficacy based on machine learning. Adv. Sci. 11, 2307245. https://doi.org/10.1002/advs.202307245.

He, M., Min, J., Kong, W., He, X., Li, J., Peng, B., 2016. A review on the pharmacological effects of vitexin and isovitexin. Fitoterapia 115, 74. https://doi.org/10.1016/j.fitote.2016.09.011.

Hwang, C.E., Kim, S.C., Kim, D.H., Lee, H.Y., Suh, H.K., Cho, K.M., Lee, J.H., 2021. Enhancement of isoflavone aglycone, amino acid, and CLA contents in fermented soybean yogurts using different strains: Screening of antioxidant and digestive enzyme inhibition properties. Food Chem. 340. https://doi.org/10.1016/j.foodchem.2020.128199.

Iqbal, N., Khan, N.A., Ferrante, A., Trivellini, A., Francini, A., Khan, M.I.R., 2017. Ethylene role in plant growth, development and senescence: interaction with other phytohormones. Front. Plant Sci. 08. https://doi.org/10.3389/fpls.2017.00475.

Juan, C.A., Pérez De La Lastra, J.M., Plou, F.J., Pérez-Lebeña, E., 2021. The chemistry of reactive oxygen species (ROS) revisited: outlining their role in biological macromolecules (DNA, Lipids and Proteins) and induced pathologies. Int. J. Mol. Sci. 22 (9). https://doi.org/10.3390/ijms22094642.

Kalim, M.D., Bhattacharyya, A., Banerjee, S., Chattopadhyay, 2010. Oxidative DNA damage preventive activity and antioxidant potential of plants used in Unani system of medicine. BMC Complement. Med. Ther. 10, 77. https://doi.org/10.1186/1472-6882-10-77.

Khole, S., A Panat, N., Suryawanshi, P., Chatterjee, S., Devasagayam, T., Ghaskadbi, S., 2016. Comprehensive assessment of antioxidant activities of apigenin isomers: vitexin and isovitexin. Free Radic. Antioxid. 6 (2), 155. https://doi.org/10.5530/fra.2016.2.5.

Kim, I.-S., 2021. Current perspectives on the beneficial effects of soybean isoflavones and their metabolites for humans. Antioxidants 10, 1064. https://doi.org/10.3390/antiox10071064.

Kim, J.H., Jeong, Y.J., Lee, Y.H., Shah, A.B., Kim, C.Y., Park, K.H., 2023. 1-Aminocyclopropane-1-carboxylic acid enhances phytoestrogen accumulation in soy plants (*Glycine max* L.) by its acceleration of the isoflavone biosynthetic pathway. J. Agric. Food Chem. 71, 10393–10402. https://doi.org/10.1021/acs.jafc.3c01810.

Kim, J.H., Shah, A.B., Lee, Y.H., Baiseitova, A., Ban, Y.J., Park, K.H., 2022. Changes in secondary metabolites in soybean (*Glycine max* L.) roots by salicylic acid treatment and their anti-LDL oxidation effects. Front. Plant Sci. 13. https://doi.org/10.3389/fpls.2022.1000705.

Kim, D.H., Yang, W.T., Cho, K.M., Lee, J.H., 2020. Comparative analysis of isoflavone aglycones using microwave-assisted acid hydrolysis from soybean organs at different growth times and screening for their digestive enzyme inhibition and antioxidant properties. Food Chem. 305, 125462. https://doi.org/10.1016/j.foodchem.2019.125462.

Kobayashi, M., Ohta, Y., 1983. Induction of stress metabolite formation in suspension cultures of *Vigna angularis*. Phytochemistry 22 (5), 1257–1261. https://doi.org/10.1016/0031-9422(83)80235-0.

Lee, J.H., Cho, D.Y., Jang, K.J., Jeong, J.B., Lee, G.Y., Jang, M.Y., Son, K.H., Lee, J.H., Lee, H.Y., Cho, K.M., 2023. Changes in nutrient components and digestive enzymatic inhibition activities in soy leaves by ethephon treatment. Plants 12 (20). https://doi.org/10.3390/plants12203640.

Lee, H.Y., Cho, D.Y., Kim, D.H., Park, J., Jeong, J.B., Jeon, S.H., Lee, J.H., Ko, E.J., Cho, K.M., Lee, J.H., 2024a. Examining the alterations in metabolite constituents and antioxidant properties in mountain-cultivated ginseng (*Panax ginseng* C.A. Meyer) organs during a two-month maturation period. Antioxidants 13 (5). https://doi.org/10.3390/antiox13050612.

Lee, Y.H., Kim, J.H., Baiseitova, A., Shah, A.B., Im, S.Y., Kim, J.Y., Lee, Y.B., Park, K.H., 2024d. Selective induction of furanocoumarins in *Angelica acutiloba* roots by signaling molecule, ethylene and their monoamine oxidase inhibition. Ind. Crop Prod. 213. https://doi.org/10.1016/j.indcrop.2024.118418.

Lee, H.Y., Kim, H.S., Kim, M.J., Seo, Y.H., Cho, D.Y., Lee, J.H., Lee, K.Y., Jeong, J.B., Jang, M.Y., Lee, J.H., Lee, J., Cho, K.M., 2024c. Comparison of primary and secondary metabolites and antioxidant activities by solid-state fermentation of *Apios americana* Medikus with different fungi. Food Chem. 461. https://doi.org/10.1016/j.foodchem.2024.140808.

Lee, H.Y., Lee, J.H., Cho, D.Y., Jang, K.J., Jeong, J.B., Kim, M.J., Lee, G.Y., Jang, M.Y., Lee, J.H., Cho, K.M., 2024b. Changes in nutritional compositions and digestive enzyme inhibitions of isoflavone-enriched soybean leaves at different stages (drying, steaming, and fermentation) of food processing. Food Chem. X 24. https://doi.org/10.1016/j.fochx.2024.101999.

Leite Milião, G., Hanke de Oliveira, A.P., de Souza Soares, L., Rodrigues Arruda, T., Nascif Rufino Vieira, E., de Castro Leite, B.R., 2022. Unconventional food plants: nutritional aspects and perspectives for industrial applications. Future Foods 5, 100124. https://doi.org/10.1016/j.fufo.2022.100124.

Li, S., Leng, Y., Feng, L., Zeng, X., 2013. Involvement of abscisic acid in regulating antioxidative defense systems and IAA-oxidase activity and improving adventitious rooting in mung bean [*Vigna radiata* (L.) Wilczek] seedlings under cadmium stress. Environ. Sci. Pollut. 21 (1), 525. https://doi.org/10.1007/s11356-013-1942-0.

Li, N., Xu, J., Zhao, Y., Zhao, M., Liu, Z., Wang, K., Huang, J., Zhu, M., 2024. The influence of processing methods on polyphenol profiling of tea leaves from the same large-leaf cultivar (*Camellia sinensis* var. *assamica* cv. Yunkang-10): nontargeted/targeted polyphenomics and electronic sensory analysis. Food Chem. 460. https://doi.org/10.1016/j.foodchem.2024.140515.

Lu, Y., Chang, X., Guo, X., 2019. Dynamic changes of ascorbic acid, phenolics biosynthesis and antioxidant activities in mung beans (*Vigna radiata*) until maturation. Plants 8 (3). https://doi.org/10.3390/plants8030075.

Mcsteen, P., Zhao, Y., 2008. Plant hormones and signaling: common themes and new developments. Dev. Cell 14 (4), 467. https://doi.org/10.1016/j.devcel.2008.03.013.

Park, M., Baek, S., Park, S., Yi, J., Cha, S., 2023. Comparative study of the mechanism of natural compounds with similar structures using docking and transcriptome data for

improving *in silico* herbal medicine experimentations, 2023 Brief. Bioinform. 24 (6), 1–12. https://doi.org/10.1093/bib/bbad344.

Petrine, J.C.P., Del Bianco-borges, B., 2020. The influence of phytoestrogens on different physiological and pathological processes: an overview. Phytother. Res. 35 (1), 180. https://doi.org/10.1002/ptr.6816.

Pisoschi, A.M., Pop, A., 2015. The role of antioxidants in the chemistry of oxidative stress: a review. Eur. J. Med. Chem. 97, 55. https://doi.org/10.1016/j.ejmech.2015.04.040.

Qu, X., Hall, B.P., Gao, Z., Schaller, G.E., 2007. A strong constitutive ethylene-response phenotype conferred on Arabidopsis plants containing null mutations in the ethylene receptors *ETR1* and *ERS1*. BMC Plant Biol. 7 (1). https://doi.org/10.1186/1471-2229-7-3.

Sathasivam, R., Kim, N.S., Lim, J., Yang, S.H., Kim, B., Park, H.W., Kim, J.K., Park, S.U., 2025. Comprehensive analysis of primary and secondary metabolites and antioxidant activities provides insights into metabolic profiling of different organs of *Pimpinella brachycarpa* Naka. Food Chem. 468, 142394. https://doi.org/10.1016/j.foodchem.2024.142394.

Selwal, N., Rahayu, F., Herwati, A., Latifah, E., Supriyono, Suhara, C., Kade Suastika, I. B., Mahayu, W.M., Wani, A.K., 2023. Enhancing secondary metabolite production in plants: exploring traditional and modern strategies. J. Agric. Food Res. 14. https://doi.org/10.1016/j.jafr.2023.100702.

Shen, N., Wang, T., Gan, Q., Liu, S., Wang, L., Jin, B., 2022. Plant flavonoids: classification, distribution, biosynthesis, and antioxidant activity. Food Chem. 383, 132531. https://doi.org/10.1016/j.foodchem.2022.132531.

Silva, L.R., Pereira, M.J., Azevedo, J., Gonçalves, R.F., Valentão, P., De Pinho, P.G., Andrade, P.B., 2013. *Glycine max* (L.) Merr., *Vigna radiata* L. and *Medicago sativa* L. sprouts: A natural source of bioactive compounds. Food Res. Int. 50 (1), 167. https://doi.org/10.1016/j.foodres.2012.10.025.

Tripathi, A., Chauhan, N., Mukhopadhyay, P., 2024. Recent advances in understanding the regulation of plant secondary metabolite biosynthesis by ethylene-mediated pathways. Physiol. Mol. Biol. Plants 30 (4), 543. https://doi.org/10.1007/s12298-024-01441-w.

Van de Poel, B., Smet, D., Van Der Straeten, D., 2015. Ethylene and hormonal cross talk in vegetative growth and development. Plant Physiol. 169 (1), 61–72. https://doi.org/10.1104/pp.15.00724.

Vaseva, I.I., Qudeimat, E., Potuschak, T., Du, Y., Genschik, P., Vandenbussche, F., Van Der Straeten, D., 2018. The plant hormone ethylene restricts *Arabidopsis* growth via the epidermis. PNAS 115 (17). https://doi.org/10.1073/pnas.1717649115.

Wójciak, M., Drozdowski, P., Ziemlewska, A., Zagórska-Dziok, M., Nizioł-Łukaszewska, Z., Kubrak, T., Sowa, I., 2024. ROS Scavenging effect of selected isoflavones in provoked oxidative stress conditions in human skin fibroblasts and keratinocytes. Molecules 29 (5). https://doi.org/10.3390/molecules29050955.

Xiao, Y., Fan, J., Chen, Y., Rui, X., Zhang, Q., Dong, M., 2016. Enhanced total phenolic and isoflavone aglycone content, antioxidant activity and DNA damage protection of soybeans processed by solid state fermentation with *Rhizopus oligosporus* RT-3. RSC Adv. 6 (35), 29741. https://doi.org/10.1039/c6ra00074f.

Xie, C., Park, K.H., Kang, S.S., Cho, K.M., Lee, D.H., 2020. Isoflavone-enriched soybean leaves attenuate ovariectomy-induced osteoporosis in rats by anti-inflammatory activity. J. Sci. Food Agric. 101 (4), 1499. https://doi.org/10.1002/jsfa.10763.

Yin, Y., Liu, C., Yang, Z., Fang, W., 2023. Ethephon promotes isoflavone accumulation in germinating soybeans by its acceleration of isoflavone biosynthetic pathway. Plant Physiol. Biochem 201. https://doi.org/10.1016/j.plaphy.2023.107805.

Yoo, D.Y., Jung, S., Kang, J.S., Baek, J.H., Park, K.H., Lee, D.H., Kang, S.S., Kim, H.J., 2022. Isoflavone-enriched soybean leaves (Glycine max) alleviate cognitive impairment induced by ovariectomy and modulate PI3K/Akt signaling in the hippocampus of C57BL6 mice. Nutrients 14 (22). https://doi.org/10.3390/nu14224753.

Yoo, H.S., Lee, J.S., Kim, C.Y., Kim, J., 2004. Flavonoids of *Crotalaria sessiliflora*. Arch. Pharm. Res. 27 (5), 544–546. https://doi.org/10.1007/BF02980129.

Yu, X., Xu, Y., Yan, S., 2021. Salicylic acid and ethylene coordinately promote leaf senescence. J. Integr. Plant Biol. 63 (5), 823. https://doi.org/10.1111/jipb.13074.

Zhang, A., Fu, L., Zuo, F., 2022. HPLC analysis of vitexin and isovitexin content changes during mung bean germination. J. Food Meas. Charact. 16, 3302–3309. https://doi.org/10.1007/s11694-022-01376-4.

Zhou, Y., Gao, Y., Zhang, B., Yang, H., Tian, Y., Huang, Y., Yin, C., Tao, J., Wei, W., Zhang, W., Chen, S., Zhou, Y., Zhang, J., 2024. Cellulose synthase-like C proteins modulate cell wall establishment during ethylene-mediated root growth inhibition in rice. Plant Cell 36 (9), 3751. https://doi.org/10.1093/plcell/koae195.